Quaternary Science Reviews 222 (2019) 105904

Contents lists available at ScienceDirect

Quaternary Science Reviews

journal homepage: www.elsevier.com/locate/quascirev

Holocene glacier fluctuations on the northern flank of Cordillera Darwin, southernmost South America

B.L. Hall [a, *], T.V. Lowell [b], G.R.M. Bromley [a, c], G.H. Denton [a], A.E. Putnam [a]

[a] School of Earth and Climate Sciences and the Climate Change Institute, University of Maine, USA
[b] Department of Geology, University of Cincinnati, USA
[c] School of Geography and Archaeology, NUI Galway, Ireland

ARTICLE INFO

Article history:
Received 7 May 2019
Received in revised form
24 August 2019
Accepted 27 August 2019
Available online xxx

Keywords:
Cordillera Darwin
Holocene
Glacial extent
Radiocarbon
Chronology

ABSTRACT

Records of past variability afford context for evaluating present-day glacier behavior and for testing hypotheses of climate change. Here, we use 69 radiocarbon dates of wood and other organic materials in association with glacial deposits to document the behavior of Ventisqueros Marinelli and Brooks in Cordillera Darwin over the past ~17,000 years. Recession from the last glacial maximum was early, with most occurring prior to 17,000 yr BP. Any glacial resurgence during the Antarctic Cold Reversal must have terminated within the bounds of Holocene ice fluctuations. By early Holocene time, Ventisquero Marinelli had retreated such that it was no more extensive than it was in AD 1992. We identify several subsequent glacier readvances, but also note long periods of restricted ice extent, particularly in the mid-Holocene. There were times when Holocene glaciers must have been smaller than at present. Our new record from Marinelli shows similarities to other reconstructions of Holocene glacier variation from southern South America, such as at Mt. Sarmiento and the South Patagonian Icefield, suggesting an underlying climate signal. The overall implication is of substantial early Holocene deglaciation followed by repeated advances interspersed with periods of recession when ice extent was smaller than at present. This general pattern of glacier behavior appears to differ from that of New Zealand's Southern Alps and points to the value of a geographic spread of datasets to elucidate the pattern of Southern Hemisphere climate during the Holocene.

1. Introduction and background

Proxy records afford insight into the pattern, severity, mechanisms, and timing of natural variability necessary to develop an understanding of Holocene climate change. Various mechanisms, including changes in solar output (e.g., Denton and Karlén, 1973), deep-ocean circulation (e.g., Broecker, 1998), and volcanic activity (e.g., Miller et al., 2012), are among the proposed causes of Holocene climate change. However, an understanding of the global geographic footprint of climate variability is necessary for assessing these and other candidates for Holocene millennial- and centennial-scale climate change.

The long-term trend over the present interglacial appears to be one of summer cooling in the Northern Hemisphere and warming in at least parts of the Southern Hemisphere. This difference is demonstrated in the glacial records from the European Alps and the Southern Alps of New Zealand. In the European Alps, glacier termini were inboard of their present-day positions for much of the early and middle Holocene, as shown by radiocarbon ages of wood fragments emerging from retreating ice (Hormes et al., 2001; Joerin et al., 2006; Ivy-Ochs et al., 2009; Schimmelpfennig et al., 2012). Glacier expansion to Neoglacial positions occurred shortly after ~5000 years ago (Simmoneau et al., 2014), with subsequent intervals of expansion separated by intervals of recession. The Northern Hemisphere Little Ice Age began at approximately AD 1300 (Holzhauser and Zumbühl, 1999; Holzhauser et al., 2005), with the most extensive glacier advances culminating in the mid-1600s and mid-1800s (Holzhauser and Zumbühl, 1999; Holzhauser et al., 2005; Zumbühl and Nussbaumer, 2018). Although most clearly developed in the European Alps, this general pattern of Holocene glacier variations also has been recognized elsewhere in the Northern Hemisphere, especially in western North America (e.g., Luckman, 2000; Wiles et al., 2008).

In contrast to the situation in the north, Southern Alps glaciers

* Corresponding author.
E-mail address: brendah@maine.edu (B.L. Hall).

https://doi.org/10.1016/j.quascirev.2019.105904
0277-3791/

were more extensive at the beginning of the Holocene than at present. They appear to have undergone gradual shrinkage until the mid-Holocene, after which time they stabilized (Putnam et al., 2012). Schaefer et al. (2009) suggested that glacier fluctuations in the Southern Alps during late Holocene time were neither in phase nor out of phase with those in the European Alps.

The contrasting hemispheric pattern in long-term Holocene climate has been attributed to the opposite effects of summer insolation intensity in the Northern and Southern Hemispheres (Milankovitch, 1941). However, a recent interpretation called upon insolation-driven southward migration of the Intertropical Convergence Zone to produce northerly (warm) air flow over New Zealand that caused gradual glacier recession in the Holocene (Putnam et al., 2012). Other mechanisms, perhaps involving a bipolar seesaw through the ocean (e.g., Broecker, 1998) or atmosphere (e.g., Denton et al., 2010), could be responsible for asynchronous behavior of Northern and Southern Hemisphere glaciers on millennial timescales.

However, existing data from South America suggest that this interpretation of interhemispheric asynchrony may be too simplified. Adjacent to the South Patagonian Icefield, a date of wood from within a landslide deposit indicates that glaciers near Lago Argentino in southern South America had retreated close to present-day positions by ~9200 yr BP (Strelin et al., 2014). Thus, it is worth examining whether there are important differences in glacier behavior between southernmost South America and New Zealand during the Holocene that may reflect regional patterns of oceanic and atmospheric circulation.

To improve understanding of Holocene climate change in the Southern Hemisphere, we present here information on past glacier extents on the northern slope of Cordillera Darwin, southernmost South America (Fig. 1). Prior work on this problem in the northern Cordillera Darwin is limited. Izagirre et al. (2018) identified several moraines of presumed Holocene age, including a prominent arcuate ridge that divides the inner and outer fjord of Fiordo Marinelli, one of our field sites. We refer to this landform as "Narrows Moraine." Porter and Santana (2003) outlined the recent recession of Ventisquero (Glacier) Marinelli from Narrows Moraine, documented by aerial photographs (Fig. 2). The glacier occupied parts of the proximal slope of Narrows Moraine as recently as AD 1945. Since then, particularly since AD 1984, the glacier terminus has retreated more than 14 km. Marine sediment cores collected in Bahía Ainsworth and in Seno Almirantazgo show Holocene sedimentologic variations that have been interpreted in terms of glacial advance and retreat in the adjacent inner fjords (Boyd et al., 2008; Bertrand et al., 2017). For example, Bertrand et al. (2017) proposed episodes of glacier recession at 1200–2000 and 2700–3250 yr BP.

2. Setting

Cordillera Darwin is an east-west trending mountain range in Tierra del Fuego, with peaks that exceed 2500 m elevation. The range hosts an extensive icefield, with numerous glaciers that extend to sea level. This maritime region is characterized by pervasive westerly winds and a strong west-east precipitation gradient. Annual precipitation exceeds several meters near the Pacific coast but is only ~1–2 m at the eastern end of the range near the Argentinean border (Tuhkanen, 1992; Sagredo and Lowell, 2012). The mountains experienced heavy glacial erosion during the last glacial maximum (LGM), with scoured bedrock now widely exposed. Areas below treeline with suitable soil support dense *Nothofagus* forests (primarily *N. betuloides* and *N. antarctica)* in the central and northern regions and Magallanic moorland in the western and southern areas. The Subantarctic Front of the Southern Ocean lies only ~70 km to the south of Cordillera Darwin in the Drake Passage. Most glaciers in Cordillera Darwin retreated in the last decade, although several that descend from the highest peaks in the central Cordillera advanced briefly during the AD 2000s (Koch, 2015).

We focused on two sites in northern Cordillera Darwin – Fiordo Marinelli/Bahía Ainsworth and nearby Fiordo Brooks. Both fjords extend approximately north-south into the heart of Cordillera Darwin and have water depths generally <200 m. Ventisquero Marinelli descends northward from the main mountain divide and occupies the head of Fiordo Marinelli (Fig. 3), which, together with Bahía Ainsworth, is 21 km long. Fiordo Brooks (Fig. 4) extends more than 40 km into the mountains and displays numerous branches, each headed by glaciers, many of which terminate at tidewater.

3. Methods

We derived a record of Holocene glacier activity from 1) the ages and stratigraphic context of wood and plant remains recently exposed by retreating ice, and 2) the radiocarbon ages of the lowest organic remains in cores taken from bogs resting on glaciated terrain. Together with field surveys, we mapped glacial deposits onto satellite imagery and aerial photographs to provide context for our dates. We examined stratigraphic sections and logged the sedimentology and organic remains at 1-cm resolution. We collected samples from sections for radiocarbon dating, including wood, peat, and shells, both *in situ* and reworked. Sampling of large logs was accomplished with hand saws and electric chain saws. Where possible, rings were counted on discs to obtain minimum estimates of tree lifespan and hence ice-free conditions at, and potentially upfjord of, the sample sites. Rings generally were easily visible and counting error is thought to be minimal. The outermost preserved ring (or rings) was sampled for radiocarbon dating, and thus no correction was needed for the ontogenetic age of the tree.

All radiocarbon samples were cleaned by sonicating in distilled water. They were then dried and submitted to the NOSAMS laboratory at Woods Hole Oceanographic Institution for analysis. Ages presented in the text, except those from historical imagery, are given in calendar years with a 2-sigma error, as determined from the INTCAL13 calibration curve and CALIB 7.1 (Reimer et al., 2013). Marine samples were calculated with Marine13 and a delta R of 220 ± 40 years derived from mollusks in a fjord in southern South America (Ingram and Southon, 1996). Dates derived from historical imagery are presented as years AD. Our framework for interpreting the radiocarbon dates is presented in the Discussion.

4. Results

4.1. Ventisquero Marinelli

The Marinelli region (Fig. 3) is characterized by a wide outer fjord (Bahía Ainsworth), which is a Holocene sediment depocenter (Boyd et al., 2008), and a narrow inner fjord (Fiordo Marinelli). A prominent terminal moraine complex, "Narrows Moraine" (Figs. 3, 5B and 5C), marks the boundary between the wider and narrower fjords. In places, the moraine rests on a core of bedrock, which likely formed a natural pinning point for Ventisquero Marinelli. Since AD 1984, Ventisquero Marinelli has undergone overall retreat of ~14 km. Until AD 1945, the terminus remained on the proximal slope of Narrows Moraine complex (Porter and Santana, 2003, Fig. 2). This multi-crested, composite landform (Izagirre et al., 2018) crosses the inner fjord mouth with only a narrow opening of less than 2 m water depth at high tide. This opening restricts water exchange with the outer fjord and prevents icebergs from escaping from the inner fjord. The present-day glacier has receded largely onto land, although minor portions still calve into the fjord. The

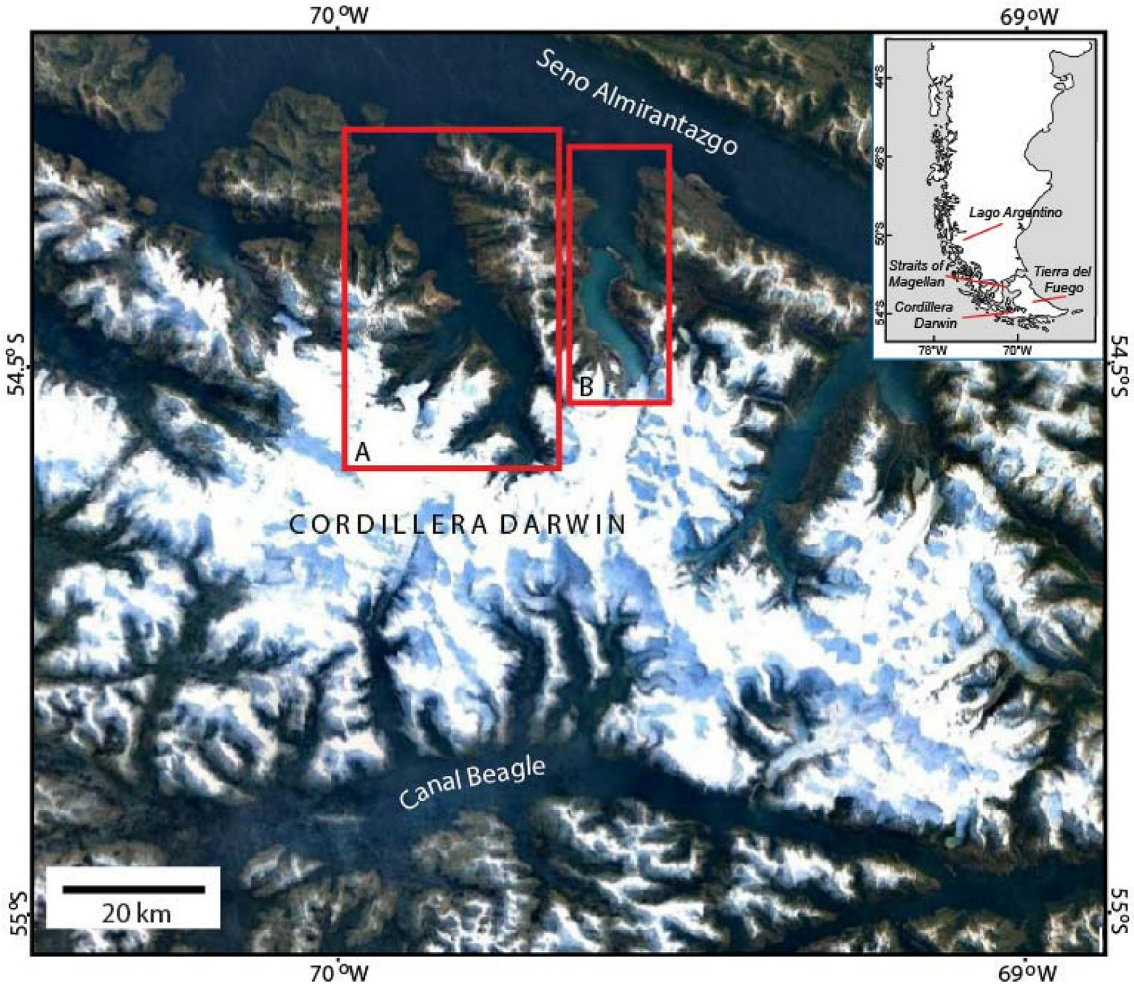

Fig. 1. Index map of Cordillera Darwin, with inset of southern South America. Red boxes refer to the principle field areas in this study, including Fiordo Brooks (A) and Fiordo Marinelli (B). Imagery from Google Earth. (For interpretation of the references to colour in this figure legend, the reader is referred to the Web version of this article.)

inner fjord is typically less than 160 m deep and shows considerable bottom topography (Koppes et al., 2009). The wall on the east side of the fjord is covered with unstable, ice-cored drift that extends to a prominent trimline at about 100 m elevation (Fig. 5A and D). Lateral valleys (V1–V4) open to the more gently sloping west side of the fjord (Fig. 3), and relict shorelines document past ice-marginal lakes that formed as the glacier advanced and then drained as the glacier retreated.

Inboard of Narrows Moraine, ancient wood is common in drift on the lower slopes of the fjord (Fig. 6) and in sections containing both glacial and non-glacial sediments. Sixty-nine radiocarbon dates of wood, peat, and shells (Table 1) indicate that there were several times during the Holocene when the inner fjord was at least partly free of ice. Ring counts indicate that some trees were at least 200 years old (Table 2). Ages of glacially transported wood range from ~400 to 8270 yr BP, spanning most of the Holocene. We report here on stratigraphic sections and sampling localities, all of which are close to sea level. All sites are shown on Fig. 7 (keyed to site numbers in Table 1) and all sections are described here and detailed more thoroughly in the Supplemental Information (Figs. S1–S11).

4.1.1. Section 11

Section 11 occurs close to sea level distal to Narrows Moraine on the north side of the narrow east arm of the fjord (Figs. 7, 8, S4). A thin layer of *in situ* peat overlies a compact silty diamicton that contains pieces of wood. The lower boundary of the peat afforded an age of 1130 ± 60 yr BP (OS-56697), and wood within the diamicton dated to 1320 ± 40 yr BP (OS-56441).

4.1.2. Section 17

A section on the west side of the fjord displays three units, all diamictons (Figs. 7, 9, S8, S9). Reworked wood within the lowest diamicton dates to 8270 ± 90 yr BP (OS-61475) and that in the middle deposit yielded a similar age of 7830 ± 100 yr BP (OS-63947). The upper unit, a strongly deformed silt-rich diamicton, contains abundant transported wood and broken shells. A single date of wood is 6650 ± 90 yr BP (OS-64098), whereas a broken shell yielded an age of 7570 ± 70 yr BP (OS-64850).

4.1.3. Section 24

Section 24 occurs on the east side of the fjord ~8.5 km inboard of Narrows Moraine (Fig. 7). This section consists of stratified deltaic and fan sediments derived from a side-valley stream, overlain by tills (Figs. 10, S2, S3). Rare *in situ* mollusks (*Aulacomya*), of which only the organic portions are preserved, occur in the lowest exposed sediments. Overlying well-sorted sand and gravelly sand contains leaf detritus and small pieces of reworked wood. A layer of *in situ* peat rests on the gravels and is, in turn, overlain by till. This till contains abundant large pieces of reworked wood. Our interpretation of this site (see Supplemental Information for more

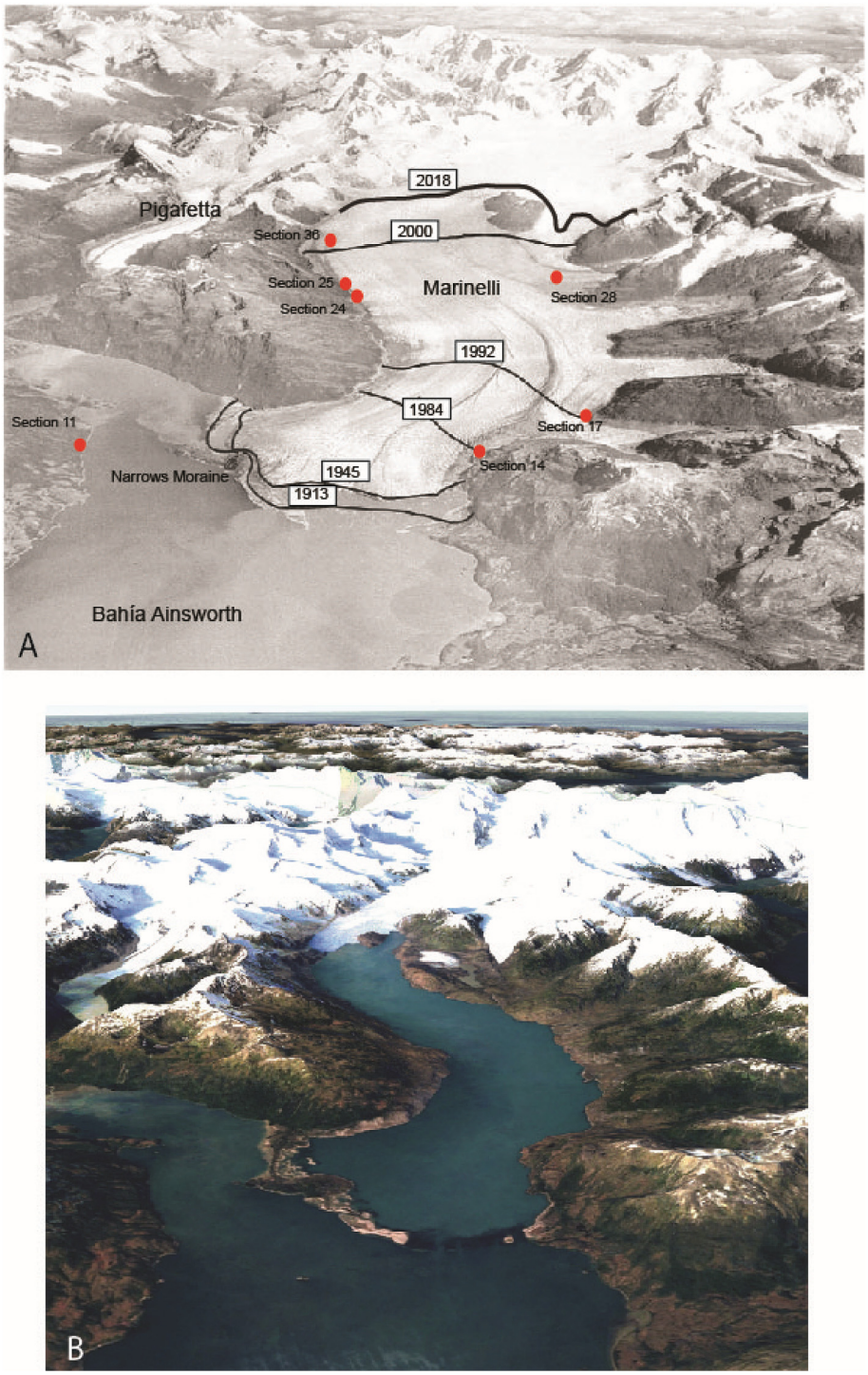

Fig. 2. A. US Air Force photograph (AD 1945) of Ventisquero Marinelli, with ice positions modified after Porter and Santana (2003). Red dots show locations of sections in this study. B. Present-day view of Ventisquero Marinelli from Google Earth imagery. View in both images is to the south. (For interpretation of the references to colour in this figure legend, the reader is referred to the Web version of this article.)

detail) is that it represents remnants of an alluvial fan deposited at the edge of the fjord from a lateral valley. This fan subsequently was overrun at least once by Ventisquero Marinelli. Dates obtained from wood and shells within the fan sediments yielded ages of ~4000 yr BP (shells: 3840 ± 120 yr BP, OS-57855; wood: 4190 ± 110 yr BP, OS-56439; 4040 ± 110 yr BP, OS-56639; 4060 ± 90 yr BP, OS-56445). *In situ* peat overlying the fan sediments afforded ages of 2850 ± 80 yr BP (OS-57891) and 3210 ± 70 (OS-56440) yr BP (top and bottom of peat layer, respectively). Expansion of the glacier is indicated by the diamicton at the top of the section, which contains transported wood dating both to 1330 ± 40 (OS-56637) and to 740 ± 50 (OS-57857) yr BP (Table 1).

4.1.4. Section 25

Along the eastern wall of the fjord, till mantles a bedrock outcrop, which we refer to as Section 25 (Figs. 7 and S7).

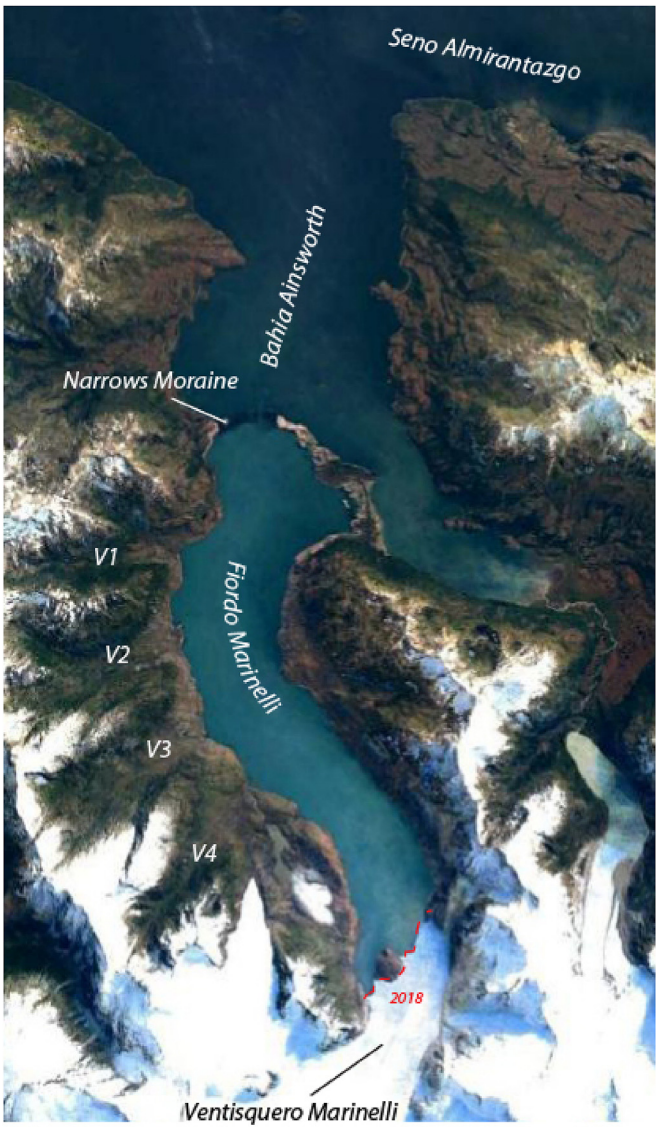

Fig. 3. Location map of the Marinelli region (B on Fig. 1) with key features indicated. The AD 2018 ice marginal position is drawn in red. V1–V4 refer to Valleys 1 through 4. Imagery from Google Earth. (For interpretation of the references to colour in this figure legend, the reader is referred to the Web version of this article.)

Immediately upglacier of this bedrock knob, numerous logs, some from trees nearly 200 years old and many aligned parallel to the long axis of the fjord, litter the landscape (Fig. 6B). Relict soil and forest floor material also are present. The wood is splintered, with glacial silt filling many cracks, but is not significantly deformed. Bark is preserved on some wood pieces. In addition, some pieces of wood have been pushed into the adjacent bedrock (Fig. 6A). Ten dates of wood lodged within the till and bedrock cavities range from ~400 to 710 yr BP. Two additional dates of forest litter are 300 ± 20 (OS-56724) and 400 ± 60 (OS-56726) yr BP. Loose wood on the till surface yielded two ages of 390 ± 80 (OS-56728) and 700 ± 30 (OS-56729) yr BP. In addition, fragments of shells collected within diamicton exposed ~8 m lower in elevation than the main section dated to 3360 ± 100 yr BP (OS-57559).

4.1.5. Section 28

In Valley 4, lacustrine sediments overlying till form the base of Section 28, located ~30 m above sea level (Figs. 7, 11, S10, S11). These sediments are overlain by *in situ* peat and then by coarsening-upward gravel. The peat and gravel are overlain by a second lacustrine silt unit, and then by a diamicton unit. Leaf fragments at the base of the peat yielded an age of 3910 ± 80 yr BP (OS-61535). Compressed wood in the lower gravel unit dates to 3650 ± 70 (OS-61333) and 3530 ± 80 (OS-63928) yr BP. Detrital wood at the base of the upper lake bed unit dates to 2430 ± 80 yr BP (OS-64097). Our interpretation of this section is that an advance of Ventisquero Marinelli blocked the mouth of the lateral valley, causing the formation of an ice-marginal lake. Shorelines of such lakes are common in Valleys 1–4 (e.g., Izagirre et al., 2018). Retreat of the glacier caused the lake to drain, allowing the growth of peat. A glacier readvance was accompanied by deposition of outwash, followed by deposition of additional lake beds as Marinelli ice again sealed off the valley mouth. Continued ice advance led to deposition of the diamicton that caps the section.

4.1.6. Section 36

Section 36 extends for more than 50 m along the eastern wall of the fjord. It displays at least four units, each with abundant glacially transported wood. Some trees were more than 100 years old when they died (Figs. 6E and F, 7, 12, S5, S6). The lower unit displays orange-stained, stratified and sorted sand and gravel beds with scattered cobble clasts. One of the abundant pieces of wood within this unit produced an age of 5400 ± 80 yr BP (OS-56640). In the northern end of the section, this unit is overlain by a wedge of gravelly diamicton, also bearing pieces of reworked wood, one of which dates to 4690 ± 80 yr BP (OS-56442). Extending along the length of the section is a ~50 cm thick clast-supported layer of bouldery, cobbly diamicton. The upper unit, a gray silty diamicton, lies on the clast-supported layer and exhibits numerous large glacially molded stones and abundant clasts of wood and peat. Two pieces of wood produced ages of 3790 ± 100 and ~3850 yr BP. In AD 2006, Section 36 was located within a few hundred meters of the glacier front.

4.1.7. Bog cores

To constrain the maximum possible Holocene ice extent, we cored several bogs near sea level resting on glacial deposits outboard of Narrows Moraine (Fig. 7). At the mouth of the outer fjord (7 km outboard from Narrows Moraine), six samples taken from within a few centimeters of the contact between organic sediments and the underlying glacial rock flour, range from ~16,000 to 17,000 yr BP (Hall et al., 2013). On the west side of the outer fjord, 3 km outboard of Narrows Moraine, three different bogs yielded basal ages of 3450 ± 110 (OS-104079), 13,160 ± 90 (OS-104187), and 15,680 ± 340 (OS-104093) yr BP for the lowest organic materials. On the east side of the fjord, the base of the hillside peat yielded ages of 1260 ± 40 (OS-56999) and 5820 ± 90 (OS-56484) yr BP. In the east arm of the fjord closer to Narrow Moraine, two samples of the lowest organic materials in bogs dated to 3090 ± 90 (OS-104080) and 4350 ± 100 (OS-104078) yr BP.

4.2. Fiordo Brooks

Brooks (Figs. 4 and 13) is a major fjord situated to the west of Fiordo Marinelli. It extends more than 40 km into Cordillera Darwin, splitting into two arms (Brazos Este and Oeste), the eastern of which splits yet again. Glaciers occur at the head of each arm. Fjord walls are steep, and glacial deposits are difficult to locate because of dense tree cover.

We examined deposits adjacent to two glaciers in Fiordo Brooks. In Brazo Este, the eastern glacier (here referred to as Brooks Este 2; Figs. 4 and 14A) now terminates on bedrock at the high tide mark. Aerial photographs from AD 1945 show an expanded glacier that

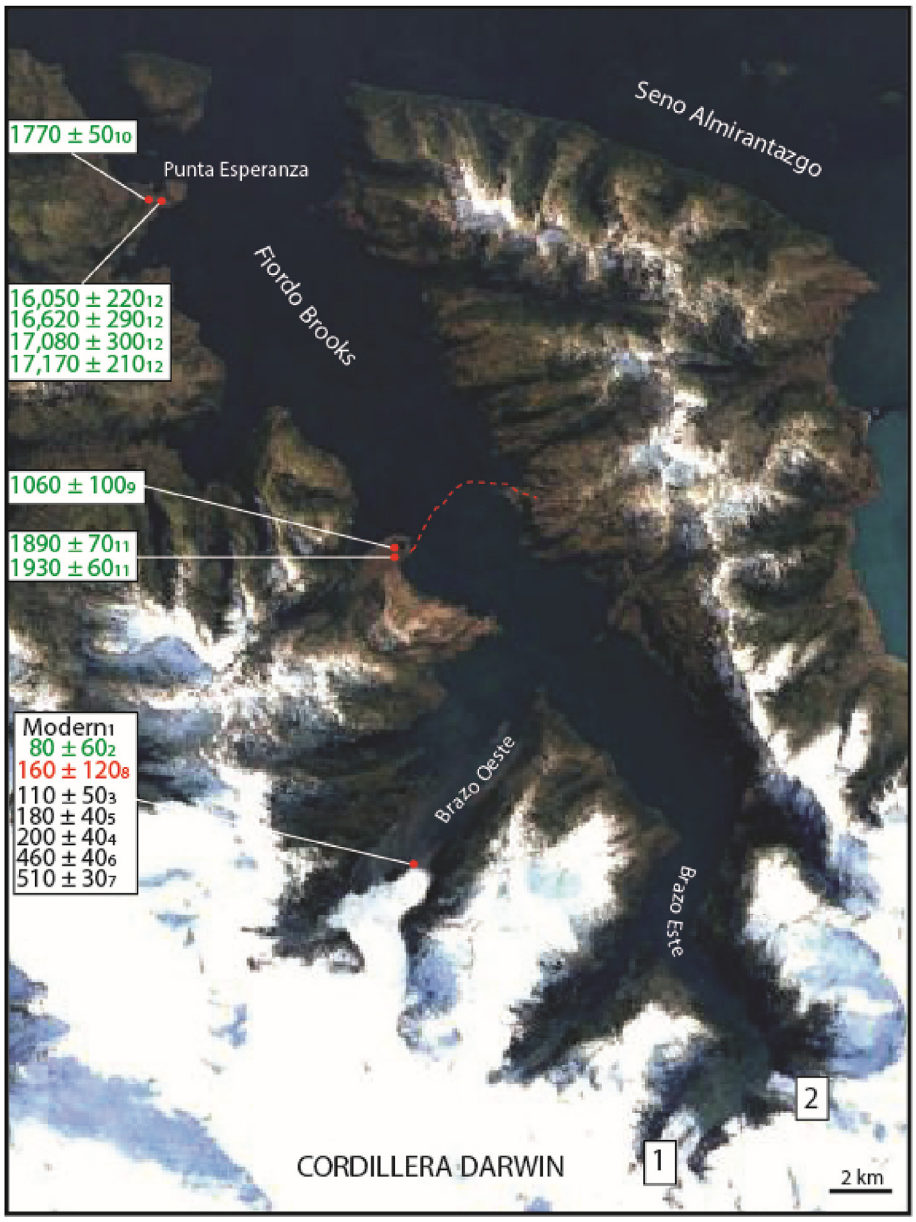

Fig. 4. Location map of the Brooks region (A on Fig. 1) with key features and calibrated radiocarbon dates indicated. Dates are keyed to Table 3 with subscripts. Black dates are of transported wood. Red dates are of shells. Green dates are of *in-situ* organic remains in bog cores. "Modern" (sample 1) refers to a sample that cannot be calibrated because it dates close to or after AD 1950.1 = Brooks Este 1 Glacier. 2 = Brooks Este 2 Glacier. Red dashed line shows position of possible moraine. (For interpretation of the references to colour in this figure legend, the reader is referred to the Web version of this article.)

extended laterally ~200 m to what is now a distinct trimline. Oscillating retreat since then has produced a series of small, discontinuous ridges, each approximately 10–50 cm high.

We also examined the glacier in Brazo Oeste, which is anchored on a nunatak and currently is undergoing slow advance on a shallow bank (Fig. 14B). About half of the ice front currently terminates on land against a composite moraine complex. Aerial photographs taken in AD 1945 show the glacier in about the same position as at present (Fig. 13). Past advance and then oscillating retreat have left a series of push moraines, ranging from heavily vegetated to unvegetated, on the nunatak (Fig. 14C–F). There are at least four distinct unvegetated moraines, the outermost of which shows stained clasts. Reworked wood is common in the moraines and is also scattered on the drift surface; it ranges in age from modern (in the present moraine) to 510 ± 30 yr BP (OS-57886, Table 3). Rare shell fragments in the unvegetated drift date to 160 ± 120 yr BP (OS-57560). The ice-distal flank of the vegetated moraine displays trees that have been pushed by the glacier, with some surviving. A pushed (and killed) tree (40 cm diameter) yielded a radiocarbon age that, when calibrated, is imprecise; it most likely dates to the 19th or 20th century. *N. betuloides* trees a few tens of meters distal to the moraine reach more than 85 cm in diameter and nearly 300 cm in circumference at breast height.

About halfway between the mouth and head of Fiordo Brooks, a small bedrock protrusion covered with sediment on the west side of the fjord appears to mark a former ice pinning point (Fig. 4). Together with a similar protrusion on the opposite side of the fjord and several islands, shallow bathymetry suggests that a submerged moraine crosses the fjord at this location (Fig. 4). The lowest organic material from two bogs superimposed on this feature on the west

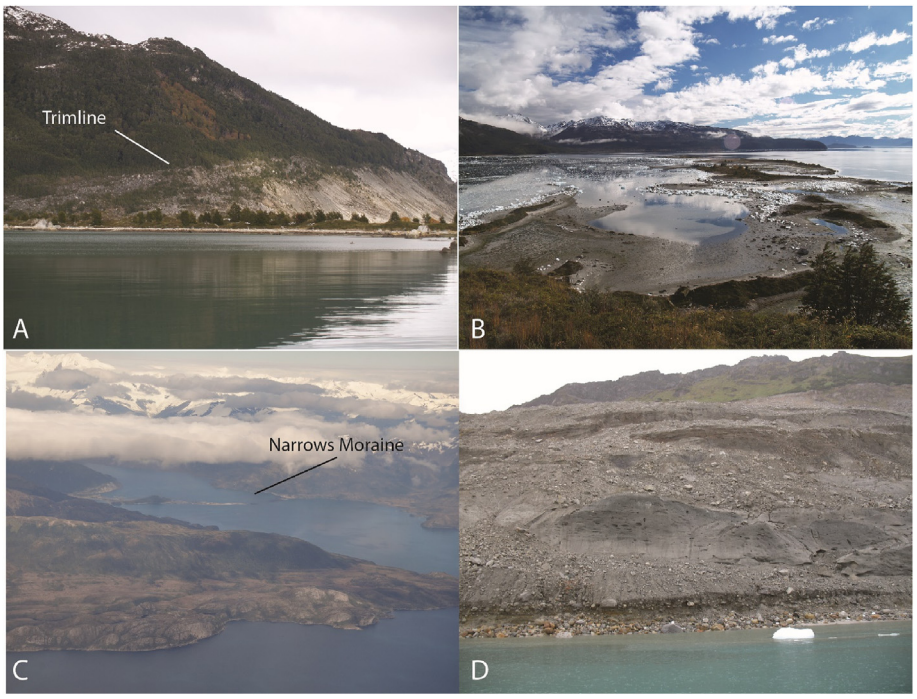

Fig. 5. Photographs from the Marinelli region. A) A prominent trimline in the inner fjord marks the ice position held until retreat in the last few decades. B) View across the gap in Narrows Moraine. C) Oblique aerial view to the south of Seno Almirantazgo (foreground), Bahía Ainsworth, Narrows Moraine, and Fiordo Marinelli. D) Unvegetated fjord walls exposed by recent retreat of Ventisquero Marinelli. The walls are covered with drift, ice-cored in places, that contains abundant organic remains.

side of the fjord yielded radiocarbon ages of ~1060 ± 100 and 1930 ± 60 yr BP.

We cored two bogs near the fjord mouth at Punta Esperanza. A shallow upland bog yielded a basal age of only 1770 ± 50 yr BP (OS-119401; Fig. 4; Table 3). A deeper bog produced ages, in stratigraphic order, ranging from 17,170 ± 210 (OS-119140) to 16,050 ± 220 (OS-61551) yr BP in the lowest meter of sediment (Hall et al., 2013 and this paper). The oldest date affords a minimum-limiting constraint on the timing of deglaciation following the LGM.

5. Discussion

5.1. Framework for interpretation of radiocarbon dates

We interpret radiocarbon ages of wood samples as follows. Unless specifically indicated otherwise (e.g., wood in fan sediments in Section 24), we assume that sampled wood pieces were transported to their collection locations by Ventisqueros Marinelli and Brooks. Most wood pieces fall into what we classify as Group 1. They are heavily splintered and show ductile deformation, with cracks packed full of silt and stones. Many of these pieces are also abraded. Although splintering can occur in both green and dry wood, green wood tends to fail ductilely by shear and stretching of fibers, rather than by abrupt cross-grain fracture typical of wood with low moisture content (Koehler, 1933; Conrad et al., 2003; Özden et al., 2017). Thus, we infer that wood samples with fibrous, elongated splinters likely were sourced from trees killed by glacier ice. Thus, such wood samples afford dates for ice advance, as well as maximum-limiting ages for the sediments in which they now occur. In most cases, the source trees grew at an unknown distance up valley from the sample collection sites. In a few cases, however, we suggest that the trees were killed close to the sample site, because the wood retains bark and/or delicate twigs and occurs together with ripped-up soil and leaves. We think it unlikely that such wood samples could have survived extensive reworking, and thus we infer that the glacier transport distance probably was short. Wood samples with these characteristics commonly are concentrated on the upglacier flank of bedrock knobs. In summary, Group 1 dates provide ages of glacial advance (tree death) and mark the end of a period of ice-free conditions at or upfjord of their collection sites.

The remaining wood samples fall into what we classify as Group 2. These samples commonly show evidence of heavy abrasion and lack the splintering and ductile deformation shown by those in the first group (e.g., Fig. 14E). Although these samples probably were sourced from trees killed by glacier ice, we cannot be certain. They afford maximum-limiting ages for the deposit in which they now occur and could have undergone multiple cycles of glacier remobilization and transport. We use Group 1 wood samples to constrain most of our inferred glacial advances. However, some of the older advances do not have sufficient Group 1 samples, and we must rely on Group 2 wood, aided by stratigraphic context. We recognize that the precise timing of our glacial reconstructions prior to ~5000 yr BP are therefore the most speculative of this study. In summary, Group 2 samples afford maximum-limiting ages for the deposits in which they are enclosed. They also may mark the timing of glacial advance, although this conclusion is not as robust as for Group 1 samples.

Group 3 consists of those materials that can be shown unequivocally to be *in situ*, such as rooted stumps, undisturbed peat layers (both in sections and in cores), undisturbed fan and deltaic sediments, and *in situ* (and, in some cases, still living) trees (e.g., Fig. 14C) pushed over or scarred by glaciers. These samples contain information on ice-free conditions at their location and, depending upon the setting, may record the timing of ice expansion over the sample site.

A final Group 4 consists of marine mollusk shells. All such samples, whether *in situ* or not, indicate ice-free conditions at or upfjord of their current location during their time of growth.

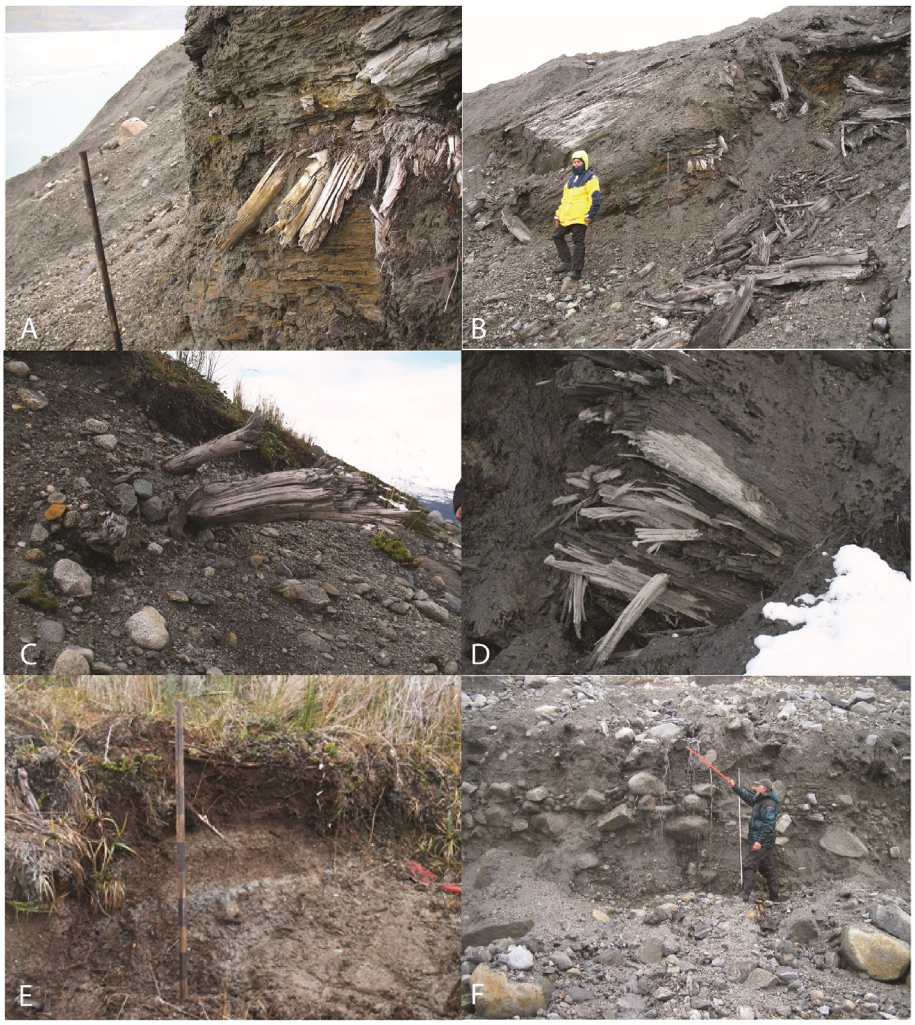

Fig. 6. Examples of glacially transported wood from Fiordo Marinelli. A) Wood thrust into bedrock at Section 25. B) Expanded view of Section 25. C) Wood at Section 14. D) Splintered wood at Section 25. E) Section 36 along the east side of Fiordo Marinelli. Stick for scale is 1.5 m tall. F) Log in till at Section 36 (person pointing to log in upper unit). Panels A–D show examples of Group 1 wood (see Discussion).

Glacially transported shells also afford maximum-limiting ages for ice expansion.

Overall, the presence of organic materials indicates times when plants (and marine mollusks) were able to grow and the fjord, at least partially, was free of glacier ice. If these organisms were killed by glacier ice, then their ages also constrain the end of that interval of ice-free conditions and the timing of ice advance. We also consider significant gaps in ages in our dataset (e.g., Joerin et al., 2006), particularly those that follow many tree deaths, to be potential times of expanded ice when trees could not grow alongside the fjord.

We note that our chronologic information constrains both the timing and the extent of Ventisquero Marinelli during the late-glacial and Holocene intervals. All sites, including peat bogs that lack evidence of glacial overriding, lie at or within a few tens of meters of sea level. We use dated materials from peat bogs (e.g., site 3) to infer that ice has never extended past those sites since organic accumulation began. We acknowledge that while it is theoretically possible that a glacier could have extended past these sites if the fjord were dry, and the glacier rested on land now 100–200 m below sea level, we find this scenario unlikely. First, there is no evidence that water level was ever significantly lower than at present in Seno Almirantazgo and Bahía Ainsworth. Deglaciation was accompanied by the presence of a lake (e.g., Bentley et al., 2005; McCulloch et al., 2005), the evidence for which is above present sea level. As there is no evidence of substantial postglacial isostatic rebound in Cordillera Darwin, we infer from those deposits that the paleo-lake surface must have been close to or above present-day sea level. Water level may have dropped temporarily when marine waters flooded the Marinelli region by 13,000 yr BP (Boyd et al., 2008), because global sea level may have been ~60 m below present (Fleming et al., 1998). However, throughout the Holocene, sea level has been close to that at present or even slightly above present (Porter et al., 1984), precluding any time of low water level that would have allowed expansion of Ventisquero Marinelli past our sites. This analysis is consistent with the geophysical and sedimentological data of Boyd et al. (2008) from the floor of Bahía Ainsworth, which lack any evidence of glacial expansion following initial deglaciation.

5.2. Deglaciation from the LGM position and the Antarctic Cold Reversal

During the LGM, glaciers from the north flank of Cordillera Darwin expanded and contributed to low-gradient ice streams that filled the Straits of Magellan and Bahía Inútil (e.g., Bentley et al.,

Table 1
Radiocarbon data from Marinelli region. Calibrations are shown as the midpoint of the range. Probabilities <10% are not shown. Numbers in column 1 correspond to sites in Fig. 7. Letters refer to specific locations in sections.*Originally published in Hall et al. (2013).

Map Key	Latitude	Longitude	Elev. (m)	Lab #	^{14}C yr BP	1σ	δ^{13}C	Cal yr BP	2σ	%	Material
1*	−54.3412	−69.5313	49	OS-63929	13,250	55	−26.4	15,930	200	100	*Ranunculus* seeds
1*	−54.3412	−69.5313	49	OS-64068	13,250	85	−19.4	15,940	270	100	Peat macrofossil
1*	−54.3412	−69.5313	49	OS-61606	13,400	85	−22.9	16,110	270	100	Sedge fragments
1*	−54.3412	−69.5313	49	OS-64070	13,650	90	−19.2	16,490	310	100	Peat macrofossil
1*	−54.3412	−69.5313	49	OS-64095	13,950	55	−21.1	16,900	250	100	Peat macrofossil
1*	−54.3412	−69.5313	49	OS-61545	14,050	70	−21.3	17,080	290	100	Gyttja
2	−54.3799	−69.6293	24	OS-104187	11,300	40	−29.3	13,160	90	100	Moss
3	−54.3806	−69.6295	18	OS-104093	13,100	100	−27.1	15,680	340	100	Moss
4	−54.3810	−69.6284	9	OS-104079	3200	50	−22.4	3450	110	100	Moss
5	−54.3941	−69.5515	14	OS-56999	1310	35	−25.9	1260	40	71	Peat macrofossil
								1200	20	29	
6	−54.3941	−69.5515	14	OS-56484	5070	35	−25.6	5820	90	100	Wood
7	−54.4158	−69.5730	1	OS-57858	135	30	−24.6	230	50	43	Dead tree, distal side of moraine; min.
								100	50	41	age outer Narrows Moraine
8	−54.4158	−69.5730	0.5	OS-56730	240	25	−23.5	290	20	65	Dead tree, distal side of moraine; min.
								160	10	30	age outer Narrows Moraine
9	−54.4158	−69.5730	0.5	OS-56731	285	30	−24.9	390	50	61	Dead tree, distal side of moraine; min.
								310	20	36	age for outer Narrows Moraine
10	−54.4158	−69.5730	1	OS-56437	290	35	−27.0	400	60	67	Dead tree, distal side of moraine; min.
								310	30	33	age for outer Narrows Moraine
11D	−54.4194	−69.5406	2.5	OS-56697	1220	30	−28.8	1130	60	78	Base of *in situ* peat above diamicton
								1230	30	22	
11C	−54.4194	−69.5406	2.5	OS-56441	1410	30	−27.2	1320	40	100	Wood in diamicton
12	−54.4303	−69.5335	20	OS-104080	2940	25	−24.3	3090	90	100	Grass
13	−54.4303	−69.5335	20	OS-104078	3940	45	−26.5	4350	100	85	Moss, grass
								4490	30	15	
14J	−54.4301	−69.6274	2.5	OS-56696	360	40	−25.2	360	50	52	15 cm dia. log in diamicton
								460	40	48	
14A	−54.4301	−69.6274	2.5	OS-56438	375	30	−24.3	460	40	61	30 cm dia. log in diamicton; splintered, no bark
								360	40	39	
14B	−54.4301	−69.6274	2.5	OS-56485	380	30	−25.4	470	40	65	10 cm dia. log in diamicton; splintered, no bark
								360	40	35	
14I	−54.4301	−69.6274	3	OS-57887	385	35	−27.0	470	40	64	15 cm dia. log in diamicton
								360	40	36	
14E	−54.4301	−69.6274	2.5	OS-56698	695	30	−25.8	660	20	77	15 cm dia. splintered stump in diamicton
								580	10	23	
14H	−54.4301	−69.6274	4	OS-57857	850	25	−25.5	740	50	100	25 cm dia. log in diamicton; splintered and worn
14K	−54.4301	−69.6274	5	OS-57892	920	30	−23.7	850	70	98	20 cm dia. log in diamicton
15	−54.4304	−69.6289	0	OS-63936	380	40	−25.6	460	40	58	50 cm dia. log with roots in till
								360	50	42	
16	−54.4313	−69.6328	0	OS-64087	1380	40	−25.3	1310	60	98	~40 cm dia. log in till
17A	−54.4420	−69.6402	2	OS-64098	5840	35	−27.3	6650	90	100	Wood from upper diamicton
17B	−54.4420	−69.6402	2	OS-64850	7230	30	−1.1	7570	70	100	Shell fragments in upper diamicton
17C	−54.4420	−69.6402	1	OS-63947	7000	40	−26.7	7830	100	100	Wood in band of wood-rich diamicton
17D	−54.4420	−69.6402	0	OS-61475	7440	45	−26.8	8270	90	100	Wood from lower diamicton
18	−54.4420	−69.6402	0	OS-61334	700	30	−27.3	670	20	82	*N. antarctica* log in till, ~40 cm dia.
								580	10	18	
19	−54.4451	−69.6425	3	OS-63946	320	30	−24.6	390	80	100	~4 m long log, ~40 cm dia., eroded out of diamicton and exposed in stream
20	−54.4451	−69.6425	3	OS-63933	360	35	−23.7	360	50	51	70 cm dia. log with rotten core in diamicton; no bark
								460	40	49	
21	−54.4451	−69.6425	4	OS-63939	380	30	−24.9	470	40	65	30 cm dia. trunk in diamicton
								360	40	35	
22	−54.4730	−69.5822	5	OS-63935	260	30	−26.1	310	30	57	Wood in diamicton
								390	40	30	
								160	10	12	
23	−54.4730	−69.5822	5	OS-61335	1770	30	−23.6	1680	70	90	Sheared stump eroding from diamicton, likely *in situ*, other stumps present
24L	−54.4737	−69.5824	0.7	OS-57885	835	30	−25.8	740	50	100	Wood in diamicton
24P	−54.4737	−69.5824	0.7	OS-56637	1420	30	−25.6	1330	40	100	Large log in diamicton
24K	−54.4737	−69.5824	0.7	OS-57891	2760	30	−27.7	2850	80	99	Top of *in situ* compressed peat layer
24J	−54.4737	−69.5824	0.7	OS-56440	3020	35	−25.2	3210	70	72	Base of *in situ* compressed peat layer
								3310	30	21	
24E	−54.4737	−69.5824	0.7	OS-56639	3700	40	−27.7	4040	110	100	Flattened small piece of wood in alluvial sediment
24F	−54.4737	−69.5824	0.7	OS-56445	3720	35	−24.8	4060	90	99	Flattened small piece of wood in alluvial sediment
24B	−54.4737	−69.5824	0.7	OS-56439	3790	40	−28.2	4190	110	94	Wood and fibrous plant material in alluvium
24A	−54.4737	−69.5824	0.7	OS-57855	4020	35	−14.6	3840	120	100	*In situ Aulacomya* periostracum 40 cm in fan
25D	−54.4775	−69.5784	10	OS-56724	250	25	−30.0	300	20	70	Forest litter plastered on bedrock
								160	10	20	
25Z	−54.4775	−69.5784	10	OS-56722	310	30	−28.0	400	60	76	Splintered wood plastered against bedrock
								320	20	24	

(*continued on next page*)

Table 1 (*continued*)

Map Key	Latitude	Longitude	Elev. (m)	Lab #	^{14}C yr BP	1σ	δ^{13}C	Cal yr BP	2σ	%	Material
25J	−54.4775	−69.5784	10	OS-56726	315	25	−26.9	400	60	78	Forest duff on top of splintered log
								320	20	22	
25A	−54.4775	−69.5784	10	OS-56723	320	25	−27.5	400	60	78	Branches plastered against bedrock, bark present
								320	20	22	
25U	−54.4775	−69.5784	10	OS-63931	320	25	−26.0	400	60	78	Wood in diamicton
								320	20	22	
25W	−54.4775	−69.5784	20	OS-56728	330	30	−26.0	390	80	100	Wood in diamicton
25T	−54.4775	−69.5784	10	OS-63940	355	30	−26.0	360	50	53	Wood in diamicton
								460	40	47	
25Y	−54.4775	−69.5784	10	OS-56721	370	30	−26.6	460	40	57	Splintered wood plastered against bedrock
								360	40	43	
25Q	−54.4775	−69.5784	10	OS-63941	435	30	−23.8	490	40	98	Wood in diamicton
25V	−54.4775	−69.5784	10	OS-63934	465	30	−26.5	510	30	100	Wood in diamicton
25M	−54.4775	−69.5784	8	OS-57884	485	25	−26.4	520	20	100	Large log with other abundant wood in gully in diamicton, bark present. All trunks dropped in same direction. Some rot in center
25L	−54.4775	−69.5784	10	OS-56725	590	20	−25.4	620	30	74	40 cm dia. log in diamicton on bedrock, at least 10 m long,
								560	10	26	some bark present, fine rings
25H	−54.4775	−69.5784	10	OS-56436	610	30	−24.9	600	50	100	Bark of log OS-56725
25X	−54.4775	−69.5784	20	OS-56729	755	30	−26.0	700	30	100	Wood in diamicton
25N	−54.4775	−69.5784	5	OS-56638	795	25	−27.8	710	30	100	Large log plastered on striated bedrock with roots present; one of many such logs all parallel to ice flow
25S	−54.4775	−69.5784	2	OS-57559	3490	35	−0.3	3360	100	100	Small, thick-shelled clam broken in till, one of many
26	−54.4753	−69.6284	3	OS-61476	280	35	−24.9	400	60	59	Large log in till, one of many
								310	30	37	
27	−54.4850	−69.6170	1	OS-62854	4570	45	1.6	4620	150	99	Broken shells in diamicton
28G	−54.4889	−69.6210	34	OS-64097	2430	25	−27.7	2430	80	75	Wood at base of lake beds
								2670	30	19	
28E	−54.4889	−69.6210	31	OS-63928	3310	30	−25.7	3530	80	100	Wood in sand layer
28D	−54.4889	−69.6210	30	OS-61333	3410	30	−28.1	3650	70	98	Compressed wood in sand layer
28A	−54.4889	−69.6210	30	OS-61535	3590	40	−28.0	3910	80	93	Leaf fragments in base of lower peat
29	−54.4983	−69.5874	4	OS-61336	365	25	−26.4	460	40	56	Wood in till beneath stagnant ice
								360	40	44	
30	−54.4983	−69.5874	4	OS-61332	380	30	−24.9	470	40	65	Wood in till beneath stagnant ice
								360	40	35	
31	−54.4983	−69.5874	4	OS-64089	425	25	−23.8	490	30	98	Wood in till beneath stagnant ice
32	−54.4983	−69.5874	4	OS-64285	430	30	−26.4	490	40	96	Wood in till beneath stagnant ice
33	−54.4983	−69.5874	4	OS-64088	455	30	−27.4	510	30	100	Wood in till beneath stagnant ice
34	−54.4983	−69.5874	4	OS-63926	505	30	−26.8	530	30	98	Wood in till beneath stagnant ice
35	−54.4983	−69.5874	4	OS-63942	535	30	−25.8	540	20	75	Wood in till beneath stagnant ice
								620	20	25	
36D	−54.5010	−69.5519	3	OS-63925	3520	35	−26.3	3790	100	100	Small tree with bark, slightly flattened in diamicton
36C	−54.5010	−69.5519	3	OS-61504	3550	35	−25.6	3820	100	98	Wood in diamicton
								3780	10	14	(replicate of OS-61622)
36C	−54.5010	−69.5519	3	OS-61622	3560	30	−26.2	3870	60	80	Wood in diamicton (replicate of OS-61504)
								3780	20	10	
36A	−54.5010	−69.5519	2	OS-56442	4190	35	−25.4	4690	80	74	Twig in diamicton
								4810	30	25	
36B	−54.5010	−69.5519	2	OS-56640	4690	40	−26.5	5400	80	85	Wood in diamicton
								5560	20	15	
37	−54.5034	−69.5830	4	OS-61477	360	25	−26.0	460	40	52	Small piece of wood with fragile branches and bark in till
								360	40	48	beneath stagnant ice
38	−54.5170	−69.5518	3	OS-112087	640	25	−24.4	580	30	58	Wood emerging from glacier in 2013
								650	20	42	
39	−54.5170	−69.5518	3	OS-112088	680	30	−26.0	660	20	64	Wood emerging from glacier in 2013
								580	20	36	

2005; Evenson et al., 2009). Surface exposure-age data at Bahía Inútil, down the glacier flowline from Cordillera Darwin (Evenson et al., 2009; Darvill et al., 2015), indicate that the LGM position was maintained until ~18,400 yr BP (McCulloch et al., 2005; Kaplan et al., 2011; Lennon, 2014; Darvill et al., 2017). Alongside Fiordo Marinelli, radiocarbon dates of the lowermost organic materials within bogs distal to Narrows Moraine indicate that glacier ice had receded to Bahía Ainsworth by at least ~17,100 yr BP (Fig. 7). This age of recession was similar to that at Fiordo Brooks, where dates from the Punta Esperanza bog indicate ice-free conditions at that site before ~17,200 yr BP (Fig. 4). These data indicate substantial deglaciation of the LGM Cordillera Darwin ice field (~85–100 km ice retreat) between ~18,400 and 17,200 yr BP during the earliest stage of Heinrich Stadial I (~17,500-14,500 yr BP), as suggested in Hall et al. (2013, 2017). Such extensive recession is consistent with rapid warming at the start of the termination in this sector of the Southern Hemisphere shortly after 18,000 yr BP.

By ~15,680 yr BP, the terminus of Ventisquero Marinelli was no more than 3 km outboard of Narrows Moraine, because the bog at Site 3 has not been overridden by ice subsequent to the start of organic deposition. As none of the bog sediments examined along Bahía Ainsworth shows evidence of overriding ice subsequent to initial deglaciation, we conclude that any readvance during the Antarctic Cold Reversal (ACR, 14,700–13,100 yr BP) must have

terminated inboard of site 38 on Fig. 7. Thus, late-glacial ice extent in this sector of Cordillera Darwin must have been comparable to that of the Holocene. We speculate that the most likely terminal position for any ACR advance of Ventisquero Marinelli was at Narrows Moraine, a composite geomorphological feature that lies on a bedrock pinning point.

5.3. Holocene history of Ventisquero Marinelli

In Fiordo Marinelli, radiocarbon dates of organic materials inboard of Narrows Moraine indicate times when ice extent was less than that of AD 1984 (Porter and Santana, 2003). Thus, our data indicate that forests grew alongside of Fiordo Marinelli at many times during the Holocene when ice was restricted compared to the 20th century. Moreover, ice extent during much of the Holocene must have been similar to or even smaller than at present. The earliest indication that the inner fjord was at least partially ice free comes from Section 17 (Fig. 7) where a date of 8270 ± 90 yr BP indicates when the glacier terminus must have pulled back at least 4.4 km inboard of Narrows Moraine (Fig. 15A). Thus, by early Holocene time, glacier extent was similar to or smaller than that in AD 1992 (Porter and Santana, 2003).

Section 17 (Figs. 7, 9, S8, S9), consisting of three compact diamicton units, contains the oldest samples collected for radiocarbon dating in the inner fjord. Sedimentologic structures suggest that the two lower units are at least partially waterlain. The upper diamicton is clay-rich and displays jointing and load structures. We interpret this deposit as a basal till. Based on the broken and worn nature of the organic remains, we infer that the dated wood and shells were transported glacially from sites farther upfjord, which must have been ice free when the organisms were living. Radiocarbon ages within the section are in stratigraphic order, with the lowest diamicton containing the oldest dated sample. All three diamictons could have been laid down during the same advance, with the upper basal till representing expansion over the site at or after ~6650 yr BP and the lower sediments being flow tills, with older reworked wood deposited from a nearby ice front. However, ages in the lower two units are similar (7830 ± 100 and 8270 ± 90 yr BP) and leave open the possibility of an advance of that age either at or upglacier of this site that was distinct from the glacier advance during which the upper till was produced. We infer that the advance associated with the upper till may have occurred shortly after ~6650 yr BP. A ~1000-yr gap in the radiocarbon ages for the inner fjord from about that time until ~5600 yr BP (Fig. 16) provides circumstantial evidence that the fjord was filled with ice. Based on these lines of evidence, we tentatively propose glacier advance shortly after 6650 yr BP that reached at least as far as Section 17 (Fig. 15B). Bathymetric and sediment thickness data for the fjord adjacent to Section 17 show relatively thick sediments, perhaps associated with a moraine or pinning point at this location (Koppes et al., 2009).

The fjord was clear of ice by 5400 yr BP, when wood grew upfjord of Section 36, only 1.8 km from the AD 2018 ice margin (Fig. 7). Thus, ice extent at 5400 yr BP and again at ~4700 yr BP must have been at least as small as at present. Subsequent expansion is indicated by the till capping Section 36, which incorporates wood and peat clasts dating to ~3800 yr BP. This wood still bears bark, suggesting that the trees may have been killed near Section 36 at or very soon after 3800 yr BP. Similarly, peat growth at Section 28, indicates that ice was still upfjord of Valley 4 at ~3910 yr BP. However, by ~3700 yr BP, this peat growth was curtailed by deposition of glaciofluvial gravels with wood fragments of that age (assuming the wood was not reworked from older deposits). The glacier continued to approach Valley 4, with the coarsening upward outwash sequence indicating its arrival. The valley mouth was sealed by ice and an ice-dammed lake formed after 2430 yr BP (Figs. 15C and S11), the age of wood at the base of the lake beds. The glacier subsequently expanded to fill Valley 4, producing the diamicton that caps the section (Fig. 11). This expansion may be reflected by the gap in the overall radiocarbon age distribution between 2400 and 1700 yr BP (Fig. 16).

We found only one *in situ* stump (dating to 1680 ± 70 yr BP; OS-61335, site 23) in the field area. Because it is uncertain if the tree was killed by ice and because we do not find transported wood of similar age, we interpret the stump simply as indicating ice-free conditions at its site (Fig. 7) just prior to 1680 yr BP. Thus, much of the fjord was ice free at this time.

Three sites (11, 16, 24; Fig. 7) preserve transported wood dating to 1300 yr BP. Two are within the inner fjord, and both contain large logs. The third, Section 11, is outboard of Narrows Moraine. In this third section, diamicton incorporates, and therefore must be either the same age or younger than, wood dating to 1320 ± 40 yr BP (OS-56441; Figs. 6E, 8, S4). *In situ* peat overlying the diamicton dates to 1130 ± 60 yr BP (OS-56697), indicating the return of ice-free conditions. If the diamicton is a till deposited by Ventisquero Marinelli, these dates point to an advance between 1130 and 1320 yr BP, as also suggested by the two other sites with wood of that age. The ice extent would have been to a position slightly outboard of Narrows Moraine but the east arm of the fjord could not have been sealed off for long, because there is no evidence of a lake having formed, at least above present-day sea level. Nor could the diamicton have been deposited by an advance of Pigafetta Glacier, which now occupies the head of the east arm of Bahía Ainsworth, because organic materials from a bog sediments situated close to sea level shows that ice has not passed through the east arm since at least ~4400 yr BP (site 13). Thus, either Marinelli glacier advanced only briefly as far as Section 11 at ~1300 yr BP, or the diamicton is of non-glacial origin. We prefer the first of these two possibilities, given that glacially transported wood of that age occurs at two additional sites. Moreover, mapping by Izagirre et al. (2018) suggests that a moraine lies close to the shore just outboard of Section 11. In addition, marine sediments between Narrows Moraine and Section 11 show a significant erosional hiatus that formed at some time prior to ~800 yr BP, which has been interpreted as a possible result of glacier advance (Boyd et al., 2008).

Most samples date to the last ~800 years. Interpretations of their ages in terms of glacial history are complicated by several possible calibrations of the radiocarbon timescale and by the presence of at least two populations of wood. To separate these populations and to determine the most likely times of ice advance, we plot the age ranges of each sample in Fig. 17. We restrict our analysis to wood killed and transported by Marinelli Glacier (Group 1). Although most samples display multiple age ranges, several (noted by large symbols) have single probable age distributions. From these distributions, which theoretically have 100% probability at a 2-sigma confidence level, we identify a younger and an older age group of wood. We take the mean and standard deviation (2σ) of each of these populations (which encompass the other less-certain ages) as most likely to represent the times of glacial advance in the fjord. The older of the two populations is 750 ± 110 yr BP. By far the largest collection of wood is associated with the mean at 480 ± 110 yr BP. Based on the apparent lack of subsequent tree growth alongside the fjord, we suggest that ice advanced through a forest at ~480 yr BP, killed the trees, and then remained on Narrows Moraine until the historically documented retreat subsequent to AD 1945. Ring counts of some trees within the younger group (Table 2) indicate ice-free conditions for as much as 200 years prior to this advance.

Because many samples dating to the last millennium occur in outcrops with wood of mixed ages, we infer that most wood

Table 2
Ring counts of dated wood keyed to Fig. 7. Samples with ">" counts have some portion of the rings that are not readable (more common) or that are missing (less common). Estimates of the year of tree birth are used to afford minimum constraints on the length of the ice-free period.

Map Key	Lab Number	Ring Count	Tree Death (Cal yr BP)	2σ	Tree Birth (Cal yr BP)
8	OS-56730	>72	290	20	>362
			160	10	>232
9	OS-56731	>18	390	50	>408
			310	20	>328
10	OS-56437	>82	400	60	>482
			310	30	>392
14A	OS-56438	45	460	40	505
			360	50	405
14B	OS-56485	69	470	40	539
			360	40	429
14E	OS-56698	>83	660	20	>750
			580	10	>663
15	OS-63936	246	460	40	706
			360	50	606
16	OS-64087	156	1310	60	1466
18	OS-61334	119	670	20	789
			580	10	699
19	OS-63946	173	390	80	563
20	OS-63933	209	360	50	569
			460	40	469
21	OS-63939	113	470	40	583
			360	40	473
22	OS-63935	90	310	30	390
			390	40	480
			160	10	250
24P	OS-56637	43	1330	40	1373
25A	OS-56723	32	400	60	432
			320	20	352
25L	OS-56725	>184	620	30	>804
			560	10	>744
25N	OS-56638	>36	710	30	>746
25Q	OS-63941	120	490	40	610
25T	OS-63940	88	360	50	448
			460	40	548
25U	OS-63931	51	400	60	451
			320	20	371
25V	OS-63934	56	510	30	566
26	OS-61476	220	400	20	620
			310	10	530
29	OS-61336	124	460	40	584
			360	40	484
30	OS-61332	100	470	40	570
			360	40	460
31	OS-64089	89	490	30	579
32	OS-64285	87	490	40	577
33	OS-64088	129	510	30	539
34	OS-63926	84	530	30	634
35	OS-63942	121	540	20	661
			620	20	74
36A	OS-56442	>59	4690	80	>4749
			4810	30	>4869
36B	OS-56640	>59	5400	80	>5459
			5560	20	>5619
36D	OS-63925	105	3790	100	3895
37	OS-61477	35	460	40	495
			360	40	395

predating ~480 yr BP was remobilized during the most recent advance. Thus, while indicating that trees were killed at ~750 yr BP, the data do not yield the location where that happened or the magnitude of the advance responsible. However, wood dating to the ~750 yr advance occurs right up to the terminus of the present-day glacier, suggesting a period of significantly reduced ice (glacier smaller than at present) just prior to that time.

In summary, the chronology and stratigraphy from Ventisquero Marinelli reveals several glacier expansions, as well as long intervals of time, beginning in the early Holocene, when ice extent may have been similar to or smaller than that of today. The earliest Holocene advance may have occurred at ≤8300 yr BP; its extent is uncertain as the only evidence comes from wood in Section 17 that could have been reworked during a later advance. A subsequent mid-Holocene advance, at ≤6650 yr BP, reached at least as far as the position of Section 17. We infer from the large gap in our ages that this expansion occurred soon after 6650 yr BP but was over by ~5400 yr BP, when the entire fjord was ice free. Minor fluctuations, confined within a few kilometers of the present-day ice margin, may have occurred in mid-to-late Holocene time, with the best documented advance beginning by ~3800 yr BP at Section 36. However, the central part of the fjord, beyond the region touched by these minor advances, remained ice free continuously from at least 4200 until 2800 yr BP, based on the stratigraphy at Section 24.

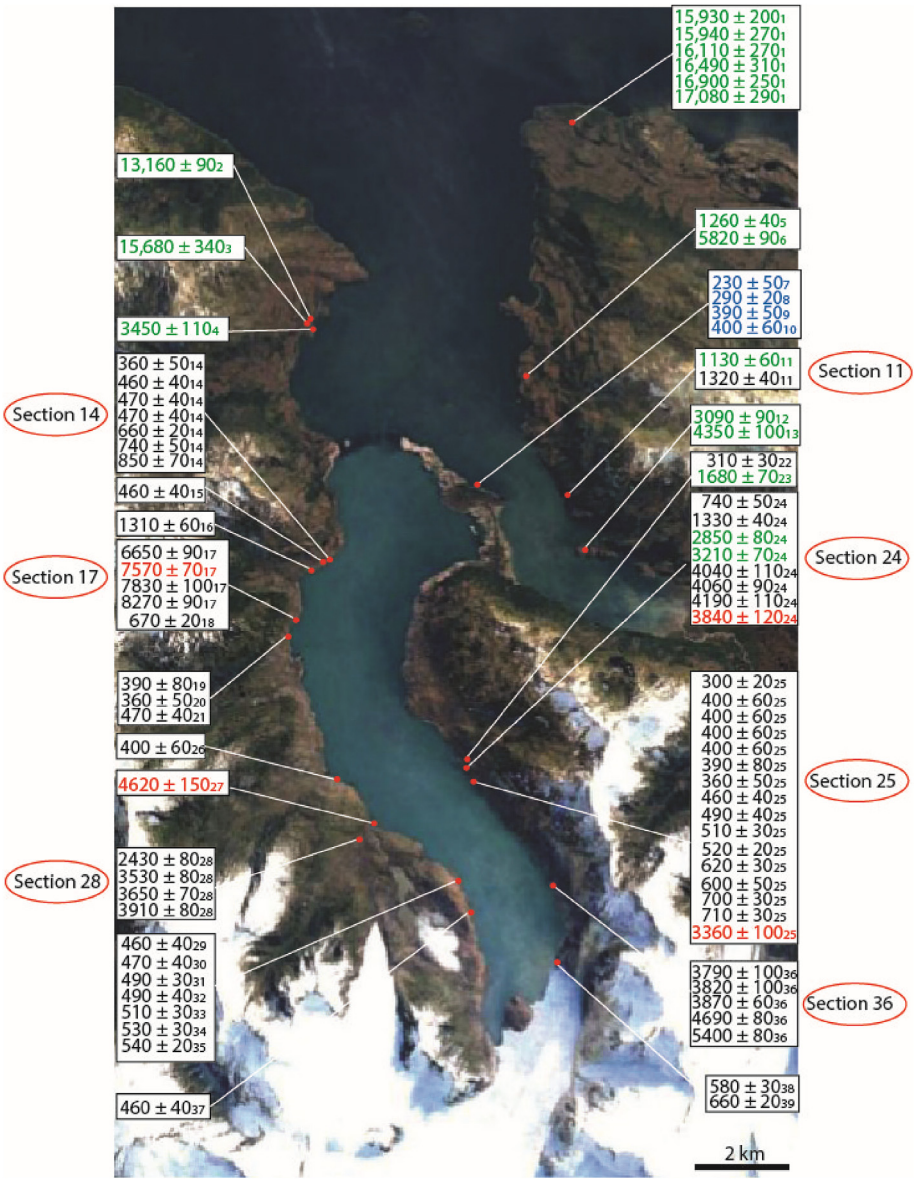

Fig. 7. Calibrated radiocarbon dates from the Marinelli region. Subscripts after dates are keyed to Table 1. Shells are denoted by red text. *In situ* deposits, mainly peat, are in green. Blue represents dead trees on the drift surface that afford only minimum-limiting ages. The remainder, in black, are of transported wood in diamicton. (For interpretation of the references to colour in this figure legend, the reader is referred to the Web version of this article.)

The advance at ~3800 yr BP appears to have been gradual, not sealing the mouth of Valley 4 until after 2460 yr BP (Section 28). A lack of dates in the range of 1700–2400 yr BP may indicate that this expansion continued, and the fjord eventually was filled with ice. Ice also advanced at ~1300 yr BP and may have extended, briefly, about 1 km beyond Narrows Moraine, although this extent remains tentative. At least two advances have occurred in the last millennium and are dated approximately to ~480 and ~750 yr BP. The most recent of these advances reached Narrows Moraine, where it remained until historical times.

5.4. Glacial history at Fiordo Brooks

Radiocarbon dates from the Punta Esperanza bog indicate that, just as at Marinelli, glaciers had receded from their LGM positions back to the mouth of the fjord by at least 17,170 yr BP. There is insufficient evidence at Brooks to determine if retreat then proceeded rapidly back to the inner reaches of the fjord. Basal ages from a bog on a pinning point/moraine halfway up the fjord are only ~1900 yr BP and may not be close minimum-limiting values for deglaciation.

The age of the youngest moraines at Brooks Oeste is better constrained. An ice-pushed tree on the distal slope of the vegetated moraine is approximately a century old (taking the most probable, but imprecise peak of the radiocarbon calibration curve). Trees on the vegetated moraine that were pushed by the glacier, but survived, may date to ~ AD 1945, when aerial photographs show glacier extent similar to that of today. Unvegetated moraines adjacent to the glacier cannot be very old, because plant colonization is rapid. The moraines must date to within the past few decades, as deposits known from photographs to have formed ~ AD 1945 today are covered with small trees. The innermost unvegetated moraine incorporates modern wood, probably killed during the most recent advance, which was underway in AD 2006. Overall,

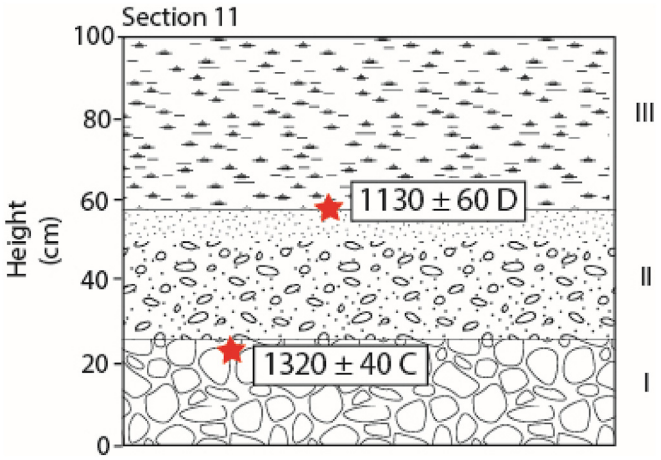

Fig. 8. Schematic diagram of Section 11 (Fig. 7). Red stars mark the location of radiocarbon samples keyed to Table 1. Roman numerals indicate stratigraphic units. Key to units is in Fig. 10. Refer to the Supplemental Information for additional details. (For interpretation of the references to colour in this figure legend, the reader is referred to the Web version of this article.)

the record at Brooks is more fragmentary than that at Marinelli, and there is insufficient evidence to make any direct correlations between the two fjords. However, both areas show similar composite moraine belts that lie in the inner fjords, and ice extended to both of these composite moraines belts in AD 1945.

5.5. Regional and hemispheric correlations

To what degree does the record from Ventisquero Marinelli reflect regional glaciation and climate? Although largely on land today, Marinelli, at times, was a tidewater glacier. Tidewater glaciers respond not only to climate, but in varying degrees, to ice dynamics related to water depth, calving, and sediment supply (Meier and Post, 1987; Alley, 1991; Pfeffer, 2007; Brinkerhoff et al., 2017). In some cases, these processes may affect only the speed and magnitude of glacial length change, but in others, glacier behavior, at least on short timescales, may be largely decoupled from climate. Pfeffer (2007) noted that tidewater glacier systems are controlled by thresholds. Long-term thinning, the result of negative mass balance, drives a glacier back across the threshold which, once crossed, leads to recession controlled largely by ice dynamics. Advance may be slower than that of a terrestrial counterpart, because of the inherent difficulty in maintaining a glacier in water. This latter problem is ameliorated by the building of sediment shoals at grounding lines (Post and Motyka, 1995; Brinkerhoff et al., 2017). Overall, tidewater glaciers may advance more slowly and retreat more rapidly than terrestrial glaciers.

Marinelli behaves as a terrestrial glacier when in the valley at the head of the fjord and when at Narrows Moraine. But to what degree do tidewater processes affect the reliability of the glacier to monitor climate when the terminus is situated between these locations? One way to assess the degree to which the Marinelli record is representative of climate-driven mass balance is to compare its history with other glacier records (preferably from terrestrial glaciers) from the region (Table 4). Is its history similar to other glaciers or is it unusual?

The glacial landforms at Fiordo Marinelli strongly resemble those of virtually every glacier in Cordillera Darwin, marine or terrestrial. Namely, Cordillera Darwin glacier termini deep within the mountain range typically are fronted by a set of tightly nested composite moraines, similar to Narrows Moraine complex. While these features at other glaciers are largely undated, based on their position and geomorphology, it is likely that they are about the same age as the composite Narrows Moraine. Where dated, bogs on terrain distal to the composite landforms (e.g., at Ventisquero Holanda, Hall et al., 2013) have yielded organic materials dating as old as ~15,000 yr BP, similar to the situation at Fiordo Marinelli. Thus, based on morphologic and geographic grounds, we infer that Narrows Moraine is similar to the composite moraines that occur throughout Cordillera Darwin.

Because of historical photographic imagery, we know that glaciers throughout Cordillera Darwin were very close to their late Holocene maximum in AD 1945. Not only was Ventisquero Marinelli banked up against Narrows Moraine, but glaciers throughout Cordillera Darwin, including the terrestrial Pigafetta Glacier adjacent to Marinelli (Fig. 2), extended onto the proximal slopes of their respective composite moraine complexes (Izagirre et al., 2018). Thus, at least for this historical event, Ventisquero Marinelli behaved in a manner compatible with that of most other Cordillera Darwin glaciers, tidewater or terrestrial.

There are only limited published sequences of dated Holocene moraines in Tierra del Fuego and adjacent areas south of the Straits

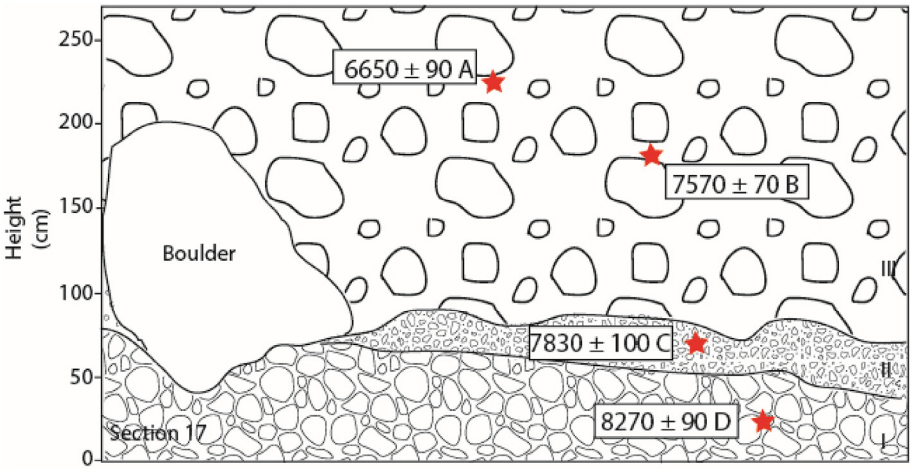

Fig. 9. Schematic diagram of Section 17 (Fig. 7). Red stars mark the location of radiocarbon samples keyed to Table 1. Roman numerals indicate stratigraphic units. Key to units is in Fig. 10. Refer to the Supplemental Information for additional details. (For interpretation of the references to colour in this figure legend, the reader is referred to the Web version of this article.)

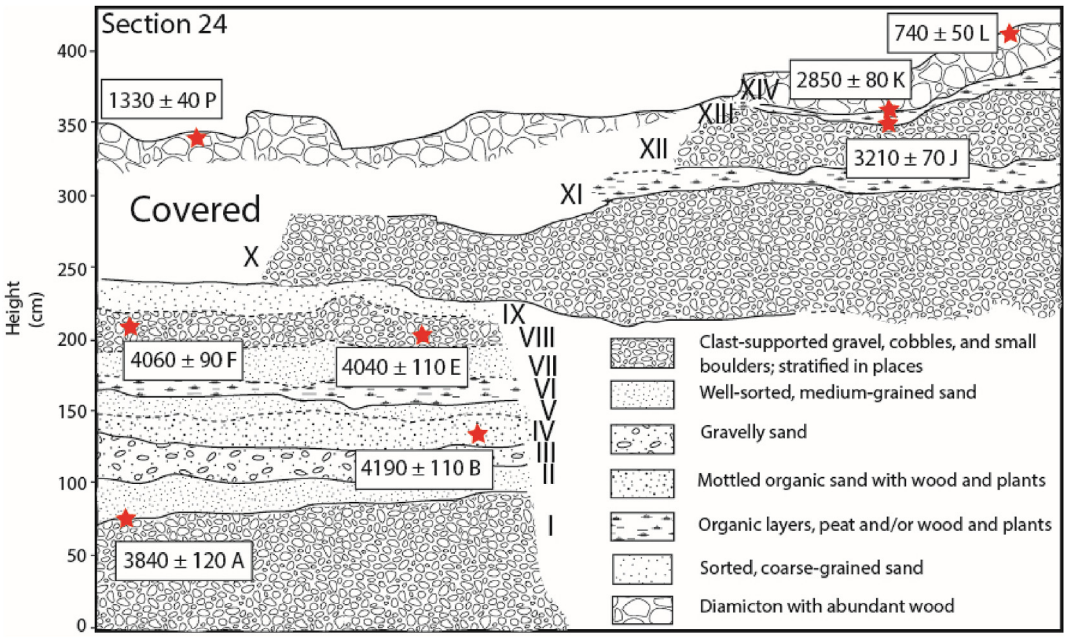

Fig. 10. Schematic diagram of Section 24 (Fig. 7). Red stars mark the location of radiocarbon samples keyed to Table 1. Roman numerals indicate stratigraphic units. Refer to the Supplemental Information for additional details. (For interpretation of the references to colour in this figure legend, the reader is referred to the Web version of this article.)

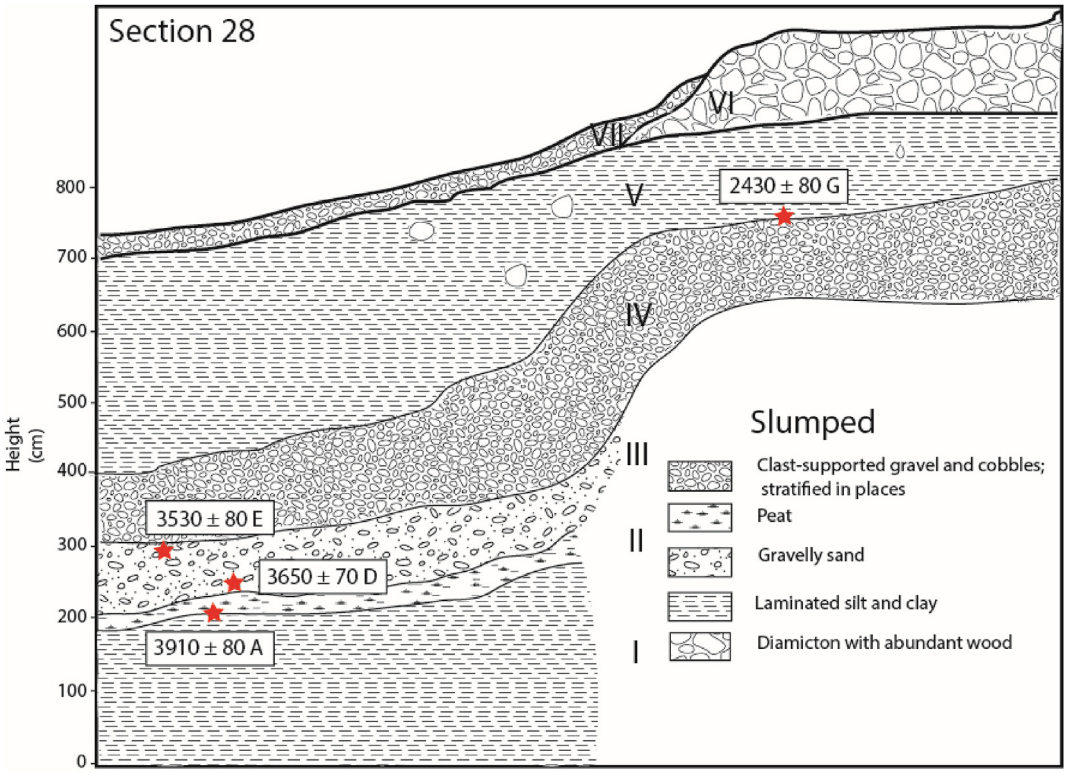

Fig. 11. Schematic diagram of Section 28 (Fig. 7). Red stars mark the location of radiocarbon samples keyed to Table 1. Roman numerals indicate stratigraphic units. Refer to the Supplemental Information for additional details. (For interpretation of the references to colour in this figure legend, the reader is referred to the Web version of this article.)

of Magellan. The most comprehensive study (Strelin et al., 2008), that from Ema Glacier, a terrestrial alpine glacier on the flank of Mt. Sarmiento (54.12°S, 71.04°W), identified a complex of inner moraines, comprising at least four advances, and a set of outer moraines. Chronology for the inner moraines came from seven dates of wood in sections. The outer moraines remain undated. A section cut through the innermost moraine shows wood in lacustrine sediments that overlie a diamicton unit. An age of 3380 ± 60 yr BP (calibrated from the original radiocarbon date) of the wood affords a minimum-limiting value for glacier advance. A second diamicton

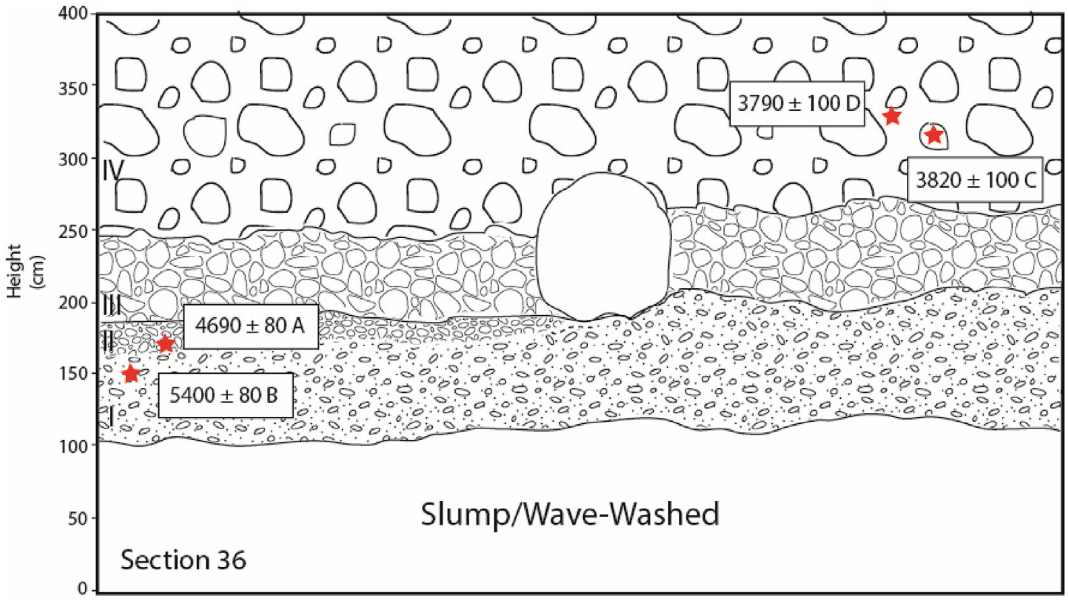

Fig. 12. Schematic diagram of Section 36 (Fig. 7). Red stars mark the location of radiocarbon samples keyed to Table 1. Roman numerals indicate stratigraphic units. Key to units is in Fig. 10. Refer to the Supplemental Information for additional details. (For interpretation of the references to colour in this figure legend, the reader is referred to the Web version of this article.)

Fig. 13. Oblique aerial view of Fiordo Brooks from AD 1945 with view north toward Seno Almirantazgo. Minimum-limiting ages for deglaciation, based on the oldest age at each site, are shown in ka. The AD 2016 ice position of Brooks Oeste is dashed in red. US Air Force Trimetrogon photograph, AD 1945. (For interpretation of the references to colour in this figure legend, the reader is referred to the Web version of this article.)

higher in the section contains wood fragments dating to, and thus younger than, 1240 ± 70 yr BP. Because the outermost ring was not dated, a correction of 27 years was applied to the date (based on ring counting), changing the age to ~1210 yr BP. The outermost moraine in the inner complex exposes two diamictons, with dates of wood of 670 ± 40 (lower) and 400 ± 60 (upper) yr BP, respectively. The younger of these ages needs to be corrected by 64 years—~340 yr BP, because the dated wood was from an inner ring. Based on preservation, Strelin et al. (2008) inferred that the trees had both been killed by the glacier and then buried immediately. Overall, they proposed advances at >3380, ≤1210, ≤670, and ≤340 yr BP. These events, particularly the latter three, are represented in the Marinelli record (Table 4), suggesting underlying climate control on these glaciers at least at centennial and greater timescales.

Menounos et al. (2013) examined moraines in the Fuegian Andes east of Cordillera Darwin. Here, leaves that overlie till just proximal to a cirque moraine were dated to 5120 ± 20 yr BP (with other similar possible calibrated ages). They also noted that the Hudson tephra, dated elsewhere to 7340–7960 yr BP (Stern, 2008), does not occur on the moraine, implying that it postdates the volcanic eruption. These data are used to bracket an advance to between ~5100 and 7340–7960 yr BP. However, the presence of tephra in some cirques to within 600 m of modern ice led them to suggest extensive deglaciation prior to the eruption in the early Holocene. Menounos et al. (2013) also identified at least two younger moraines, thought to date to the late Holocene.

The most widely cited Holocene glacial study from Tierra del Fuego is that of Kulyenstierna et al. (1996) from the Beagle Channel sector of Cordillera Darwin. From a limited number of peat cores and sections, they proposed that glaciers in Bahía Pía advanced prior to ~3000 yr BP, prior to 940 yr BP, and between 940 and 675 yr BP. No evidence was found of a Little Ice Age advance. However, upon revisiting these sections, we obtained additional dates that preclude the two younger advances, at least to the proposed extent (Hall et al., in prep.). Moreover, from a dendrochronological study near Ventisquero Italia, Koch (2015) concluded that glaciers along the Beagle Channel expanded during the Little Ice Age. Thus, at this time we exclude the Pía data from our analysis.

Both Boyd et al. (2008) and Bertrand et al. (2017) examined glacial marine sediments outboard of Fiordo Marinelli in Seno Almirantazgo. Bertrand et al. (2017) employed a variety of marine proxies from core JPC67 in Seno Almirantazgo. They did not note any pronounced changes in ice-rafted debris through the course of

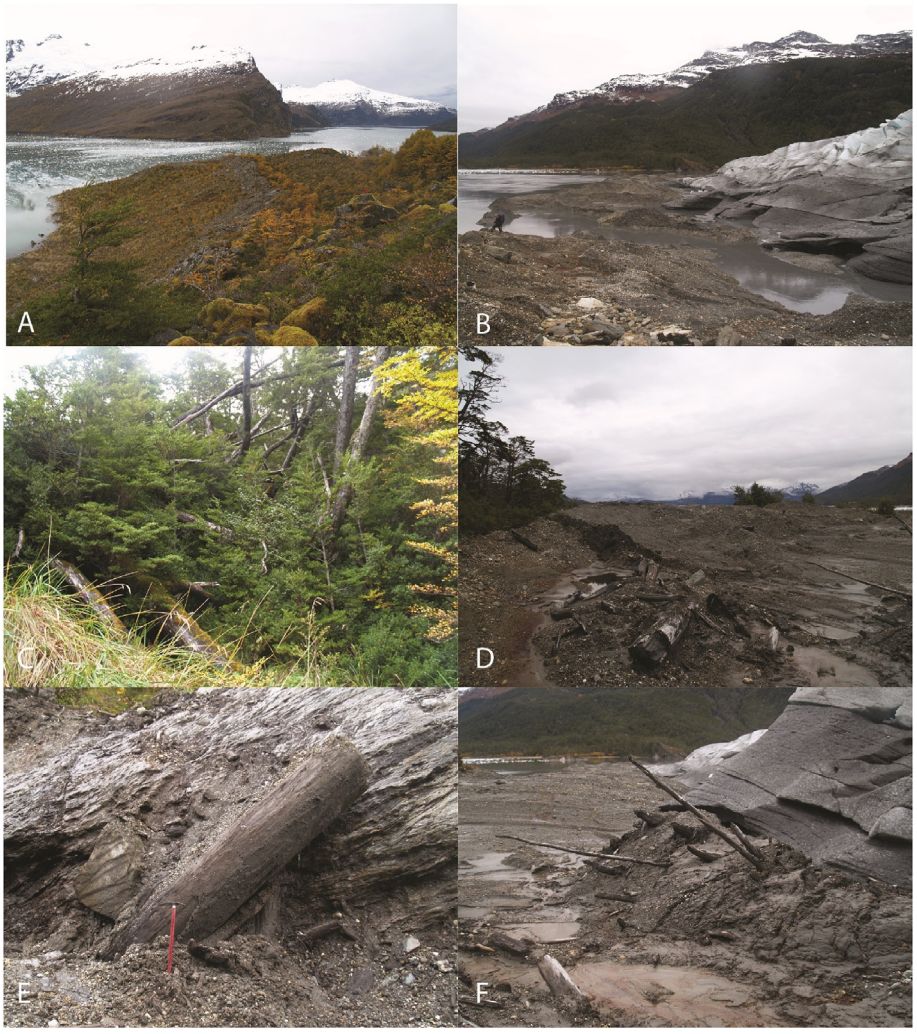

Fig. 14. Photographs from the Brooks region. A) Brooks Este 2. B) The front of Brooks Oeste, showing the moraine bank. C) Glacially pushed trees on the distal side of a moraine at Brooks Oeste. Trees in the foregound date from the late 19th or early 20th century. Trees in the background were pushed but recovered and are still alive. D) Unvegetated drift in front of Brooks Oeste. E) Lodged tree trunk exposed in recently deglaciated terrain at Brooks Oeste. F) Push moraine, likely formed during winter AD 2005.

the Holocene, a fact attributed by them to the distance icebergs would have to travel from the glaciers to the core site and to the effectiveness of shallow sills in trapping icebergs within the fjords. However, two peaks in grain size and detrital sediment input were interpreted as indicating meltwater events during Holocene glacial retreat in the inner fjords. Given uncertainties in the marine reservoir effect and in interpreting the meaning of increased terrigenous sediment input, it is difficult to compare these events with our glacial record from Marinelli. One peak in grain size, at 1200–2000 yr BP, falls just prior to the advance at ~1300 yr BP and may relate to a time of restricted ice. The other peak, at 2700–3250 yr BP, occurs during a time of reduced ice but slow glacier growth in Fiordo Marinelli.

The Marinelli record shows similarities to those from the southern part of the South Patagonian Icefield (Table 4). Based on a calibrated radiocarbon age of wood enclosed in a landslide deposit, Strelin et al. (2014) inferred extensive early Holocene deglaciation of the Agassiz Este Glacier in the Lago Argentino basin by 9200 yr BP. After an advance at 7210–7730 yr BP (Strelin et al., 2014), glaciers at Lago Argentino expanded to their maximum Holocene extent at 5000–6000 yr BP (Strelin et al., 2014; Kaplan et al., 2016). This latter event may have been replicated at Fiordo Marinelli when the glacier overrode Section 17 at $\leq$6650 yr BP (Table 4). In the late Holocene, glaciers in both locations, as well as at Torres del Paine and Mt. Sarmiento, advanced at ~1100–1400 yr BP (Aniya, 2013; Strelin et al., 2008, 2014; Kaplan et al., 2016). Likewise, glaciers in each of these locations appear to have advanced at ~600–800 and ~350–500 yr BP (Strelin et al., 2008, 2014; Kaplan et al., 2016).

One implication of the existing dataset from southern South America is that the pattern of Holocene glaciation does not resemble that of New Zealand - the only other significant mid-latitude landmass with a well-dated Holocene glacial record. Although glaciers in both Cordillera Darwin and the South Patagonian Icefield exhibit signs of significant early Holocene recession, evidence in the form of widespread wood and peat deposits emerging from beneath present-day glaciers is lacking in New Zealand's Southern Alps. Rather, glaciers there have undergone only gradual shrinkage from early until mid-Holocene time, at which time they stabilized, with minor oscillations, until the warming of the last century (Putnam et al., 2012). There is not yet any convincing evidence that Southern Alps glaciers were substantially smaller than at present at any time in the Holocene. Whether the discrepancies between the Southern Alps and southern South America glacial records stem from important

Table 3
Radiocarbon data from the Brooks region, keyed to Fig. 7. Calibrations are shown as the midpoint of the range. Probabilities <10% are not shown. #Repeat analysis. *Originally published in Hall et al. (2013).

Map Key	Sample	Latitude	Longitude	Elev. (m)	Lab #	$\delta^{13}C$	^{14}C yr BP	1σ	Cal yr BP	2σ	%	Material
Wood and Shells in Diamicton												
1	BW-10A	−54.5133	−69.8813	8	OS-57856	−26.9	modern					Bark on wood within recent moraine
2	BW-09	−54.5133	−69.8813	1	OS-57890	−25.5	95	25	80	60	73	Pushed (killed) tree on distal side of outer vegetated moraine
									240	20	27	
3	BW-10E	−54.5133	−69.8813	8	OS-56483	−24.3	140	30	110	50	38	Wood in inner unvegetated moraine
									200	30	28	
									260	20	17	
									20	20	16	
4	BW-10C	−54.5133	−69.8813	8	OS-57883	−28.5	160	30	200	40	39	Uprooted stump in inner unvegetated moraine
									270	21	18	
									*		18	
									90	30	13	
									140	10	12	
5	BWA-01	−54.5133	−69.8813	0.5	OS-57896	−23.9	190	30	180	40	59	Loose wood on drift on moraine bank
									280	20	24	
									*		17	
6	BW-10B	−54.5133	−69.8813	8	OS-56699	−25.1	370	30	460	40	57	Wood in outer unvegetated moraine
									360	40	43	
7	BW-10D	−54.5133	−69.8813	8	OS-57886	−27.3	455	30	510	30	100	Wood in outer unvegetated moraine
8	BW-10S	−54.5133	−69.8813	8	OS-57560	2.5	770	40	160	120	95	Thin, purple, broken shell inner unvegetated drift
Core Sites												
9	BI-07-02/161	−54.4224	−69.8600	2	OS-63916	−25.0	1130	40	1060	100	95	*N. betuloides* leaves in laminated silt
10	PE-13-2/83	−54.3118	−69.9520	7	OS-119401	−26.5	1830	20	1770	50	100	Peat
11	BI-07-01B/332	−54.4237	−69.8608	4	OS-61624	−25.8	1960	30	1930	60	96	*N. betuloides* leaves in laminated silt
11	BI-07-01B/332#	−54.4237	−69.8608	4	OS-61526	−26.0	1940	35	1890	70	96	*N. betuloides* leaves in laminated silt
12*	PE-07-01/14	−54.3119	−69.9490	11	OS-61551	−22.6	13,350	65	16,050	220	100	Plant macrofossils in organic silt
12	PE-13-1B T2/33	−54.3123	−69.9487	12	OS-119400	−21.7	13,750	70	16,620	290	100	Moss
12	PE-13-1 T10/14.2−14.5	−54.3123	−69.9487	12	OS-106914	−19.9	14,050	75	17,080	300	100	Moss, grass, insects
12	PE-13-1 T10/15.5	−54.3123	−69.9487	12	OS-119140	−21.9	14,100	40	17,170	210	100	Organic mud

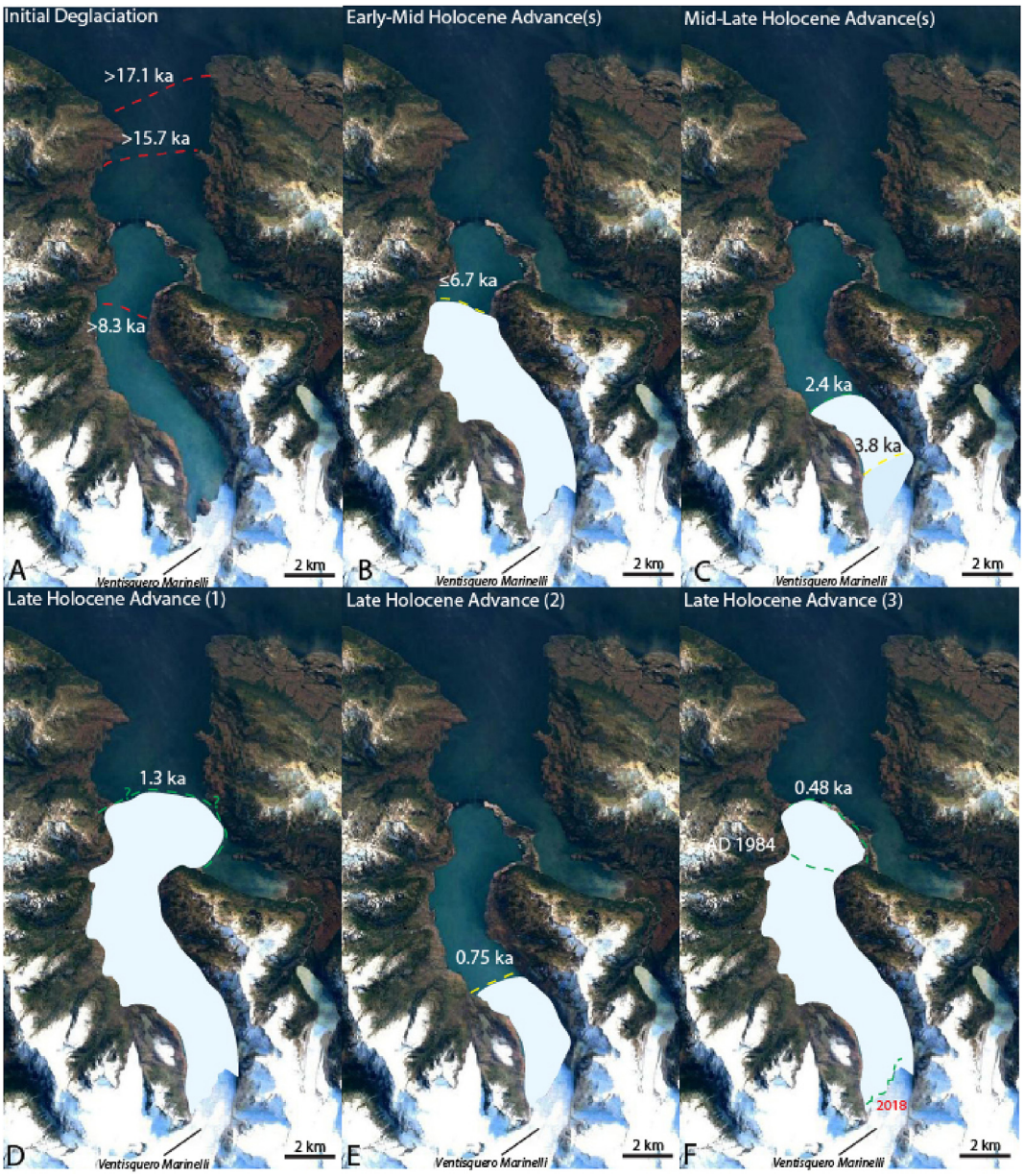

Fig. 15. Schematic diagrams depicting former ice extent in the Marinelli region. Red dashed lines indicate maximum possible ice extent; the glacier must have been behind those lines prior to the time indicated. Yellow lines indicate minimum ice extent at the time indicated; the terminus must be at or outboard of these positions. Green lines show inferred ice-marginal position. A) Initial deglaciation following the LGM, indicating maximum possible ice extent at the times given. B) Early-Mid Holocene advance. C) Mid-Late Holocene advance (two ice positions shown). The glacier may have continued to advance after 2.4 ka. D) Late Holocene advance 1. Ice at this time may have extended slightly past Narrows Moraine. E) Late Holocene advance 2. During the early part of the last millennium, ice retreated into the inner fjord and before 0.75 ka was smaller than at present. Full extent of this advance is uncertain. The depiction shown here reflects the presence of abundant logs with bark at Section 25, which we infer were killed close to their final resting place. F) Late Holocene advance 3. A robust expansion of ice to Narrows Moraine occurred at 0.48 ka. Historical imagery shows that Marinelli remained at the moraine until AD 1945 and was still close to it as late as AD 1984 (Porter and Santana, 2003). (For interpretation of the references to colour in this figure legend, the reader is referred to the Web version of this article.)

intrahemispheric differences in local climate or from the strong dependence of the South American data on glaciers that terminate in the ocean or in large lakes cannot be answered fully at present. We note that the fact that multiple South American glaciers in a variety of fjord and lake settings show the same pattern of glaciation suggests an underlying climate signal. More work is necessary, particularly on terrestrial glaciers, to refine the Holocene glacial history in southernmost South America.

6. Conclusions

Wood and other organic materials yielded 69 radiocarbon ages that constrain the past extent of Ventisqueros Marinelli and Brooks. These ages indicate that the Cordillera Darwin ice field had retreated from its LGM position to the mouth of Marinelli and Brooks fjords by ~17,000 yr BP and to within the innermost Marinelli fjord at some time between ~15,700 and 8300 yr BP. Any advance during the Antarctic Cold Reversal was of an extent similar to that of the late Holocene.

Glacially transported wood lodged in till suggests a mid-Holocene advance within Fiordo Marinelli at $\leq$6650 yr BP and possibly another at $\leq$8200 yr BP. The fjord was ice free at 5400 yr BP and remained so for much of the mid-Holocene. Increased ice extent occurred in the late Holocene, first with a small advance at

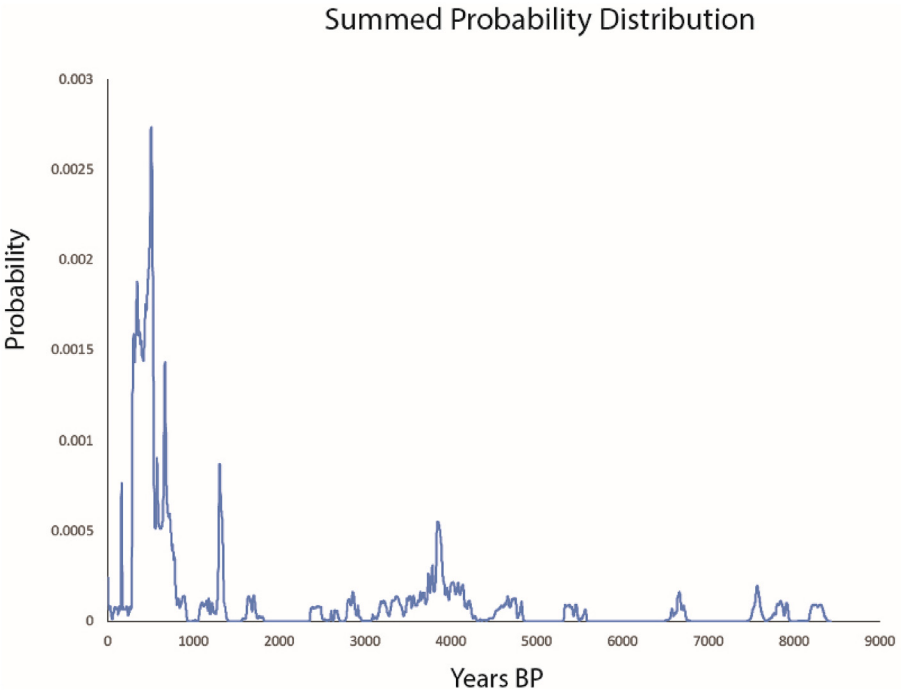

Fig. 16. Probability density plot of all radiocarbon ages proximal to Narrows Moraine. The plot is skewed heavily toward younger ages by the greater availability, multiple possible calibrations, and focused collection on wood from the youngest advance.

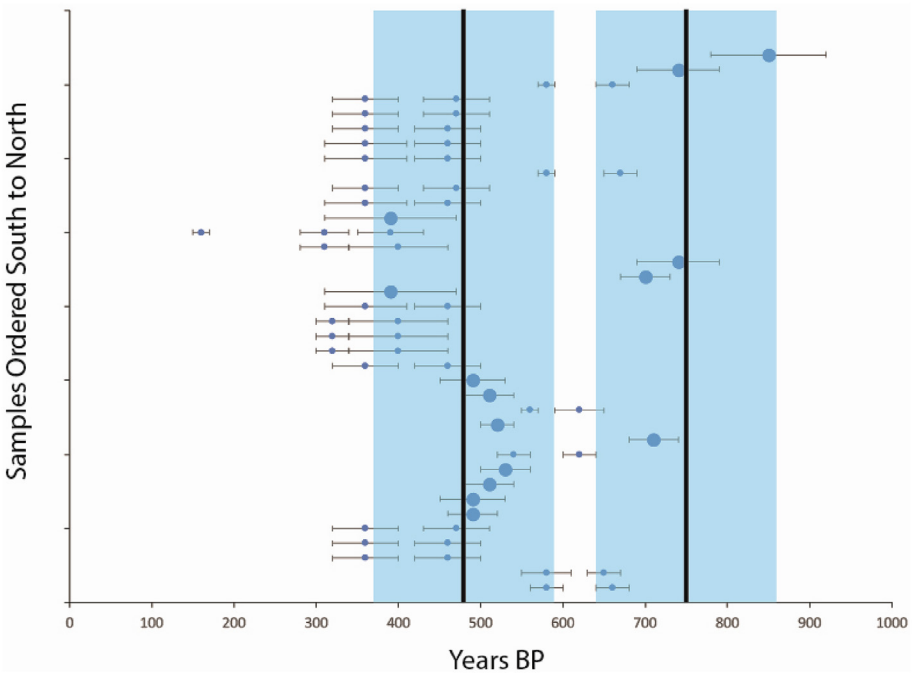

Fig. 17. Distribution of wood from the last millennium. This plot, constructed from Group 1 wood, shows 2σ calibrated age ranges of each sample, arranged from south to north. Larger symbols represent those samples with ~100% probability at the 2σ confidence interval. The mean and standard deviation (2σ) of those samples with ~100% probability are used to create the blue shaded bars, which we take as the best estimate of the ages of advance. (For interpretation of the references to colour in this figure legend, the reader is referred to the Web version of this article.)

~≤2430–3800 yr BP, followed by a greater expansion shortly after 1300 yr BP, and then at least two advances within the last millennium at ~750 and ~480 yr BP. During the last of these advances, Ventisquero Marinelli extended to Narrows Moraine.

Similar to most Cordillera Darwin glaciers (including the adjacent terrestrial glacier, Pigafetta), Ventisquero Marinelli was in an extended position, with the terminus on the proximal slope of its composite moraine, in AD 1945. Comparison of the Marinelli record with the only other comprehensive Holocene glacial chronology from the region (Ema Glacier on Mt. Sarmiento) also shows

Table 4
Correlation of glaciation in Cordillera Darwin with events at other locations in southern South America, including Mt. Sarmiento, the Fuegian Andes, and the southern South Patagonian Icefield.[1]Strelin et al. (2008);[2]Menounos et al. (2013);[3]Strelin et al. (2014);[4]Kaplan et al. (2016);[5]Aniya (2013). *Moraines of this age may exist but were not dated. #Given that radiocarbon dates in this time range commonly yield two calibrated peaks of ~480 and ~360 yr BP, some differences in age among sites may be due to timescale calibration. n.d. = no data.

Event	This Study	Mt. Sarmiento[1]	Fuegian Andes[2]	Southern SPI
Early Holocene Deglaciation	By 8300	n.d.	By 7340-7960	By 9200[3]
Advance	≤7800–8300?			7210–7730[3]
Advance	≥5400 to ≤6650	*	<7340-7960	5000–6000[3]
			>5120	6120[4]
Advance	n.d	n.d	n.d	4000–4500[5]
Advance	≤2430 to ≤3800	>3380	n.d.	3300–3600[5]
				2000–2700[3,4,5]
Advance	1130–1320	~1210	n.d.	1100–1500[3]
				1000–1450[4]
				900–1690[5]
Advance	~750	~670	*	700[3]
Advance#	~480	~340	*	>400[3]
				360[4]
Advance	n.d.	60-<340	*	<300[3]
				240[4]
				<300[5]

strong similarities, suggesting that fluctuations of Ventisquero Marinelli, although affected by tidewater processes, largely followed regional climate. The Marinelli/Ema records also resemble those from the South Patagonian Icefield.

Glacial records from southernmost South America, including that at Marinelli, differ in several critical aspects from those in New Zealand. Namely, the New Zealand records lack evidence of significant early Holocene recession and long periods of restricted ice, both of which are common features in southern South America at Marinelli and elsewhere. These differences may be attributable to the tidewater nature of many South American glaciers; however, it is also possible that there is a fundamental difference between the two locations related to local Holocene climate. In contrast, existing data from Cordillera Darwin broadly resemble the pattern of Holocene glaciation in the European Alps.

Author Credit

GHD and BLH conceived the project. BLH, GRMB, TVL, and AEP collected the radiocarbon samples. BLH performed the laboratory work, and BLH, TVL, and GHD interpreted the data. All authors contributed to writing the paper.

Acknowledgments

We dedicate this paper to the late Charlie Porter, who not only provided the logistics for this work with his boat, *Ocean Tramp*, but who also was deeply invested in the field work and the scientific results. He performed the dendrochronological analyses presented here and was instrumental in the retrieval of wood samples. A. Introne, J. Lennon, and E. Cárdenas assisted in the field. This work was funded by the U.S. National Science Foundation and by the Comer Family Foundation.

Appendix A. Supplementary data

Supplementary data to this article can be found online at https://doi.org/10.1016/j.quascirev.2019.105904.

References

Alley, R.A., 1991. Sedimentary processes may cause fluctuations of tidewater glaciers. Ann. Glaciol. 115, 119–124.
Aniya, M., 2013. Holocene glaciations of hielo patagónico (patagonia icefield), south America: a brief review. Geochem. J. 47, 97–105.
Bentley, M.J., Sugden, D., Hulton, N.R.J., McCulloch, R.D., 2005. The landforms and pattern of deglaciation in the Strait of Magellan and Bahía Inútil, southernmost South America. Geogr. Ann. 87A (2), 313–333.
Bertrand, S., Lange, C., Pantoja, S., Hughen, K., Van Tornhout, E., Wellner, J.S., 2017. Postglacial fluctuations of Cordillera Darwin glaciers (southernmost Patagonia) reconstructed from Almirantazgo fjord sediments. Quat. Sci. Rev. 177, 265–275.
Boyd, B.L., Anderson, J.B., Wellner, J.S., Fernández, R.A., 2008. The sedimentary record of glacial retreat, Marinelli Fjord, Patagonia: regional correlations and climate ties. Mar. Geol. 255, 165–178.
Brinkerhoff, D., Truffer, M., Aschwanden, A., 2017. Sediment transport drives glacier periodicity. Nat. Commun. 8 https://doi.org/10.1038/s41467-017-00095-5.
Broecker, W.S., 1998. Paleocean circulation during the last deglaciation: a bipolar seesaw? Paleoceanography 13, 119–121.
Conrad, M.P.C., Smith, G.D., Fernlund, G., 2003. Fracture of solid wood: a review of structure and properties at different length scales. Wood Fiber Sci. 35, 570–584.
Darvill, C.M., Bentley, M.J., Stokes, C.R., 2015. Geomorphology and weathering characteristics of erratic boulder trains on Tierra del Fuego, southernmost South America: implications for dating of glacial deposits. Geomorphology 228, 382–397.
Darvill, C.M., Stokes, C.R., Bentley, M.J., Evans, D.J.A., Lovell, M., 2017. Dynamics of former ice lobes of the southernmost Patagonian Ice Sheet based on a glacial landsystem approach. J. Quat. Sci. 32, 857–876.
Denton, G.H., Karlén, W., 1973. Holocene climate variations – their pattern and possible cause. Quat. Res. 3, 155–174.
Denton, G.H., Anderson, R.F., Toggweiler, J.R., Edwards, R.L., Schaefer, J.M., Putnam, A.E., 2010. The last glacial termination. Science 328, 1652–1656.
Evenson, E., Burkhart, P., Gosse, J., Baker, G., Jackofsky, D., Meglioli, A., Dalziel, I., Kraus, S., Alley, R., Berti, C., 2009. Enigmatic boulder trains, supraglacial rock avalanches, and the origin of "Darwin's boulders," Tierra del Fuego. GSA Today (Geol. Soc. Am.) 19, 4–10.
Fleming, K., Johnston, P., Zwartz, D., Yokoyama, Y., Lambeck, K., Chappel, J., 1998. Refining the eustatic sea-level curve since the Last Glacial Maximum using far- and intermediate-field sites. Earth Planet. Sci. Lett. 163, 327–342.
Hall, B., Denton, G., Lowell, T., Bromley, G., Putnam, A., 2017. Retreat of the Cordillera Darwin icefield during termination 1. *Deglaciation of the Americas from Alaska to Tierra del Fuego*. Cuadernos de Investigación Geográfica 43, 751–766.
Hall, B.L., Porter, C.T., Denton, G.H., Lowell, T.V., Bromley, G.R.M., 2013. Extensive recession of Cordillera Darwin glaciers in southernmost South America during Heinrich stadial 1. Quat. Sci. Rev. 62, 49–55.
Holzhauser, H., Zumbühl, H.J., 1999. Glacier fluctuations in the western Swiss and French Alps in the 16th century. Clim. Change 43, 223–237.
Holzhauser, H., Magny, M., Zumbühl, H.J., 2005. Glacier and lake-level variations in west-central Europe over the last 3500 years. Holocene 15, 789–801.
Hormes, A., Müller, B.U., Schlüchter, C., 2001. The Alps with little ice: evidence for eight Holocene phases of reduced glacier extent in the central Swiss Alps. Holocene 11, 255–265.
Ingram, B.L., Southon, J.R., 1996. Reservoir ages in eastern Pacific coastal and estuarine waters. Radiocarbon 38, 573–582.
Ivy-Ochs, S., Kershner, H., Maisch, M., Christl, M., Kubik, P.W., Schlüchter, C., 2009. Late pleistocene and Holocene glacier variations in the european Alps. Quat. Sci. Rev. 28, 2137–2149.
Izagirre, E., Darvill, C., Rada, C., Aravena, J.C., 2018. Glacial geomorphology of the Marinelli and Pigafetta glaciers, Cordillera Darwin icefield, southernmost Chile. J. Maps 14, 269–281.
Joerin, U.E., Stocker, T.F., Schlüchter, C., 2006. Multicentury glacier fluctuations in the Swiss Alps during the Holocene. Holocene 16, 697–704.

Kaplan, M.R., Schaefer, J.M., Strelin, J.A., Denton, G.H., Anderson, R.F., Vandergoes, M.J., Finkel, R.C., Schwartz, R., Travis, S.G., Garcia, J.L., Martini, M.A., Nielsen, S.H.H., 2016. Patagonian and south atlantic view of Holocene climate. Quat. Sci. Rev. 141, 112–125.

Kaplan, M.R., Strelin, J.A., Schaefer, J.M., Denton, G.H., Finkel, R.C., Schwartz, R., Putnam, A.E., Vandergoes, M.J., Goehring, B.M., Travis, S.G., 2011. In situ cosmogenic ^{10}Be production rate at Lago Argentino, Patagonia: implications for late-glacial climate chronology. Earth Planet. Sci. Lett. 309, 21–32.

Koch, J., 2015. Little Ice Age and recent glacier advances in the Cordillera Darwin, Tierra del Fuego, Chile, vol. 43. Annales del Instituto de la Patagonia, pp. 127–136.

Koehler, A., 1933. Causes of Brashness in Wood, vol. 342. U.S. Department of Agriculture Technical Bulletin, p. 40pp.

Koppes, M., Hallet, B., Anderson, J., 2009. Synchronous acceleration of ice loss and glacial erosion, Glaciar Marinelli, Chilean Tierra del Fuego. J. Glaciol. 55, 207–220.

Kulyenstierna, J.L., Rosqvist, G.C., Holmlund, P., 1996. Late-Holocene glacier variations in the Cordillera Darwin, Tierra del Fuego, Chile. Holocene 6, 353–358.

Lennon, J., 2014. ^{10}Be Surface-Exposure Chronology of the Trés Hermanos and Rosa Irene Moraines Near Bahía Inútil, Chilean Patagonia. M.S. Thesis. University of Maine, p. 66p.

Luckman, B.H., 2000. The little ice age in the Canadian rockies. Geomorphology 32, 357–384.

McCulloch, R.D., Fogwill, C., Sugden, D., Bentley, M.J., Kubik, P., 2005. Chronology of the Last Glaciation in the Central Strait of Magellan and Bahía Inútil, Southernmost South America. Geogr. Ann. 87A, 289–312.

Meier, M.F., Post, A., 1987. Fast tidewater glaciers. J. Geophys. Res. 92 (B9), 9051–9058.

Menounos, B., Clague, J.J., Osborn, G., Thompson Davis, P., Ponce, F., Goehring, B., Maurer, M., Rabassa, R., Coronato, A., Marr, R., 2013. Latest Pleistocene and Holocene glacier fluctuations in southernmost Tierra del Fuego, Argentina. Quat. Sci. Rev. 77, 70–79.

Milankovitch, M., 1941. Canon of Insolation and the Ice-Age Problem, vol. 132. Special Publications of the Royal Serbian Academy, p. 484.

Miller, G.H., Geirsdóttir, Á., Zhong, Y., Larsen, D.J., Otto-Bliesner, B.L., Holland, M.M., Bailey, D.A., Refsnider, K.A., Lehman, S.J., Southon, J.R., Anderson, C., Björnsson, H., Thordarson, T., 2012. Abrupt onset of the Little Ice Age triggered by volcanism and sustained by sea-ice/ocean feedbacks. Geophys. Res. Lett. 39 https://doi.org/10.1029/2011GL050168.

Özden, S., Ennos, A.R., Cattaneo, M.E.G.V., 2017. Transverse fracture properties of green wood and the anatomy of six temperate tree species. Forestry 90, 58–69.

Pfeffer, W.T., 2007. A simple mechanism for irreversible tidewater glacier retreat. Journal of Geophysical Research Earth Surface 112. https://doi.org/10.1029/2006JF000590.

Porter, C.T., Santana, A., 2003. Rapid 20th century retreat of Ventisquero Marinelli in the Cordillera Darwin icefield. An. Inst. Patagonia 31, 17–26.

Porter, S.C., Stuiver, M., Heusser, C.J., 1984. Holocene sea-level changes along the Strait of magellan and Beagle Channel, southernmost South America. Quat. Res. 22, 59–67.

Post, A., Motyka, R., 1995. Taku and Le Conte Glaciers, Alaska: calving speed control of late-Holocene asynchronous advances and retreats. Phys. Geogr. 16, 59–82.

Putnam, A.E., Schaefer, J.M., Denton, G.H., Barrell, D.J.A., Finkel, R.C., Andersen, B.G., Schwartz, R., Chinn, T.J.H., Doughty, A.M., 2012. Regional climate control of glaciers in New Zealand and Europe during the pre-industrial Holocene. Nat. Geosci. 5, 627–630.

Reimer, P., Bard, E., Bayliss, A., Beck, J.W., Blackwell, P.G., Bronk Ramsey, C., Buck, C.E., Cheng, H., Edwards, R.L., Friedrich, M., Grootes, P.M., Guilderson, T.P., Haflidason, H., Hajdas, I., Hatté, C., Heaton, T.J., Hoffmann, D.L., Hogg, A., Hughen, K.A., Kaiser, K.F., Kromer, B., Manning, S.W., Niu, M., Reimer, R.W., Richards, D.A., Scott, E.M., Southon, J.R., Staff, R.A., Turney, C.S.M., van der Plicht, J., 2013. IntCal13 and Marine13 Radiocarbon age calibration curves 0-50,000 years cal BP. Radiocarbon 55 (4), 1869–1887.

Schaefer, J.M., Denton, G.H., Kaplan, M., Putnam, A.E., Finkel, R.C., Barrell, D.J.A., Andersen, B.G., Schwartz, R., Mackintosh, A., Chinn, T., Schlüchter, C., 2009. High-frequency Holocene glacier fluctuations in New Zealand differ from the northern signature. Science 394, 622–625.

Schimmelpfennig, I., Schaefer, J.M., Akçar, N., Ivy-Ochs, S., Finkel, R.C., Schlüchter, C., 2012. Holocene glacier fluctuations in the western Alps and their hemispheric relevance. Geology 40, 891–894.

Sagredo, E., Lowell, T.V., 2012. Climatology of Andean glaciers: a framework to understand glacier response to climate change. Glob. Planet. Chang. 86–87, 101–109.

Simmoneau, A., Chapron, E., Garçon, M., Winiarski, T., Graz, Y., Chauvel, C., Debret, M., Motelica-Heino, M., Desmet, M., Di Giovanni, M., 2014. Tracking Holocene and high-altitude alpine environments fluctuations from minerogenic and organic markers in proglacial lake sediments (Lake Blanc Huez, Western French Alps). Quat. Sci. Rev. 89, 27–43.

Strelin, J.A., Kaplan, M.R., Vandergoes, M.J., Denton, G.H., Schaefer, J.M., 2014. Holocene glacier history of the Lago Argentino basin, southern patagonian icefield. Quat. Sci. Rev. 101, 124–145.

Strelin, J.A., Casassa, G., Rosqvist, G., Holmlund, P., 2008. Holocene glaciations in the Ema Glacier valley, mount sarmiento massif. Tierra del Fuego 260, 299–314.

Stern, C., 2008. Holocene tephrochronology record of large explosive eruptions in the southernmost Patagonian Andes. Bull. Volcanol 70, 435–454.

Tuhkanen, S., 1992. The climate of Tierra del Fuego from a vegetation geographical point of view and its ecoclimatic counterparts elsewhere. Acta Bot. Fenn. 125, 4–17.

Wiles, G.C., Barclay, D.J., Calkin, P.E., Lowell, T.V., 2008. Century to millennial-scale temperature variations for the last two thousand years indicated from glacial geologic records of Southern Alaska. Glob. Planet. Chang. 60, 115–125.

Zumbühl, H.J., Nussbaumer, S.U., 2018. Little Ice Age glacier history of the central and western Alps from pictorial documents. Cuadernos de Investigación Geográfica 44, 115–136.